AD-A118 774 MASSACHUSETTS INST OF TECH CAMBRIDGE AEROPHYSICS LAB F/G 20/1
DEVELOPMENT OF AN AIRBORNE SONIC THERMOMETER.(U)
SEP 82 T R CHRISTIANSEN F19628-80-K-0089
UNCLASSIFIED AFGL-TR-82-0179 NL

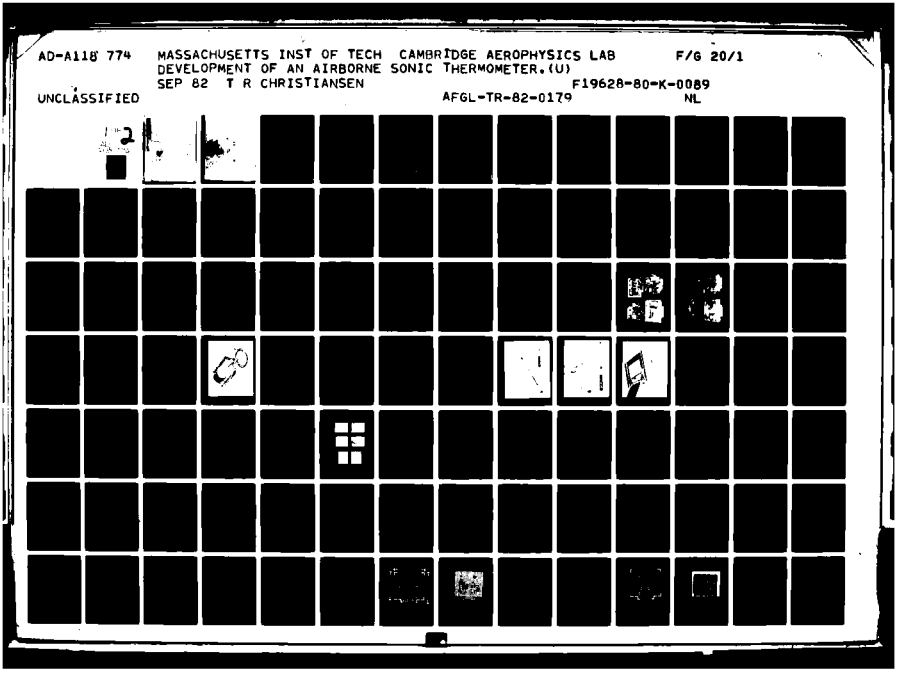

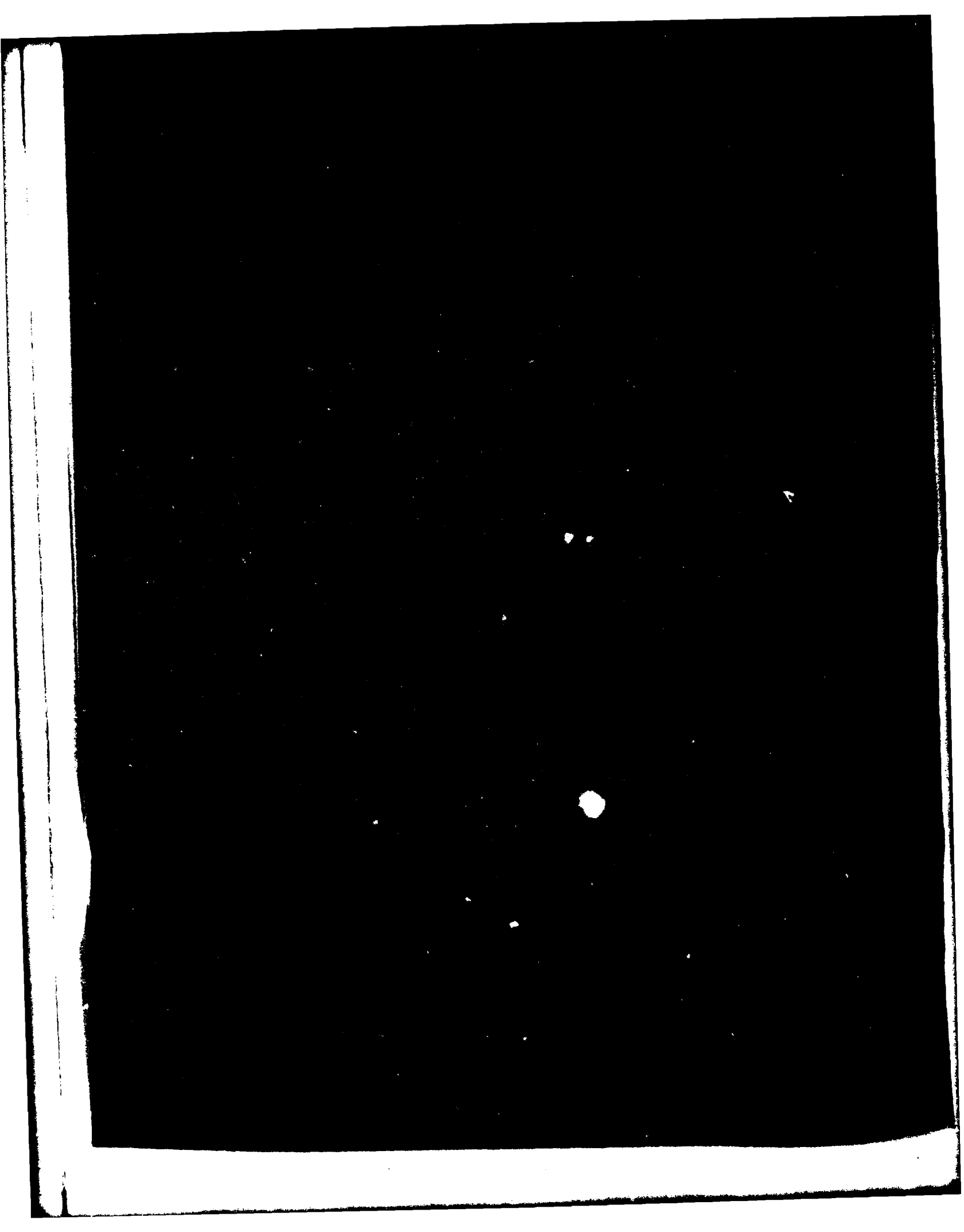

(12)

Unclassified

SECURITY CLASSIFICATION OF THIS PAGE *(When Data Entered)*

REPORT DOCUMENTATION PAGE		READ INSTRUCTIONS BEFORE COMPLETING FORM
1. REPORT NUMBER AFGL-TR-82-0179	2. GOVT ACCESSION NO. AD-A118774	3. RECIPIENT'S CATALOG NUMBER
4. TITLE *(and Subtitle)* Development of an Airborne Sonic Thermometer		5. TYPE OF REPORT & PERIOD COVERED Final Report 1 July 1980 - 30 Sept. 1982
		6. PERFORMING ORG. REPORT NUMBER
7. AUTHOR(s) Tore R. Christiansen		8. CONTRACT OR GRANT NUMBER(s) F19628-80-K-0089
9. PERFORMING ORGANIZATION NAME AND ADDRESS Aerophysics Laboratory Massachusetts Institute of Technology Cambridge, Massachusetts 02139		10. PROGRAM ELEMENT, PROJECT, TASK AREA & WORK UNIT NUMBERS 2310G3 AV
11. CONTROLLING OFFICE NAME AND ADDRESS Air Force Geophysics Laboratory Hanscom AFB, MA 01731 Monitor/Edmund A. Murphy/LKD		12. REPORT DATE September 1982 13. NUMBER OF PAGES 124
14. MONITORING AGENCY NAME & ADDRESS*(if different from Controlling Office)*		15. SECURITY CLASS. *(of this report)* Unclassified 15a. DECLASSIFICATION/DOWNGRADING SCHEDULE

16. DISTRIBUTION STATEMENT *(of this Report)*

Approved for public release; distribution unlimited

17. DISTRIBUTION STATEMENT *(of the abstract entered in Block 20, if different from Report)*

18. SUPPLEMENTARY NOTES

19. KEY WORDS *(Continue on reverse side if necessary and identify by block number)*

Acoustic thermometer
Sound speed measurement
Troposphere/stratosphere
Temperature fluctuation

20. ABSTRACT *(Continue on reverse side if necessary and identify by block number)*

An airborne sonic thermometer has been developed and is now ready for flight testing. The designed instrument uses a specially developed electromagnetic transmitter, a sensitive condenser microphone and integrated circuit components.

The air temperature is determined by measuring the phase difference between the transmitted and received signals across an acoustic path in the medium. The phase information is delivered as a changing dc-level voltage, as a digital

DD FORM 1 JAN 73 1473 EDITION OF 1 NOV 65 IS OBSOLETE

Unclassified

SECURITY CLASSIFICATION OF THIS PAGE *(When Data Entered)*

Block 20. cont'd.
signal and in the form of two phase shifted squarewaves.

Improvements of the present design are needed to exclude the effect of wind speed on the temperature measurement and in the accuracy of the calibration of the signal outputs. Once these are included, however, temperature measurements to an accuracy of plus minus one tenth of a degree centigrade, over a temperature range from plus 25°C to minus 80°C, should be available.

1. ABSTRACT

An airborne sonic thermometer has been developed and is now ready for flight testing. The designed instrument uses a specially developed electromagnetic transmitter, a sensitive condenser microphone and integrated circuit components.

The air temperature is determined by measuring the phase difference between the transmitted and received signals across an acoustic path in the medium. The phase information is delivered as a changing dc-level voltage, as a digital signal and in the form of two phase shifted squarewaves.

Improvements of the present design are needed to exclude the effect of wind speed on the temperature measurement, and in the accuracy of the calibration of the signal outputs. Once these are included, however, temperature measurements to an accuracy of plus minus one tenth of a degree centigrade, over a temperature range from plus 25°C to minus 80°C, should be available.

2. CONTENTS

LIST OF FIGURES AND TABLES

LIST OF APPENDICIES

3. INTRODUCTION

In order to study in more detail the thermal composition and the turbulence structure of the atmosphere, more accurate and time responsive thermometers would be of great value. Sonic thermometry provides a means of measuring at very short intervals, the sonic velocity of a sample of air from which the static temperature can be found. Up to an altitude of about 60 km the ideal gas approximation can be used for this. At higher altitudes a more sophisticated theory is required.

This thesis describes the results of the second year of an intended three year program undertaken by the Aerophysics laboratory at the Massachusetts Institute of Technology for the U.S. Air Force Geophysics Laboratory at Hanscomb AFB, to develop a rocket-borne sonic thermometer for use in the upper atmosphere.

Since a probe carrying rocket will ascend through the atmosphere at supersonic velocities for most of its flight path it is essential, if good spatial resolution is to be obtained, that the rate of data aquisition be very high. Also, by measuring a property of the undisturbed air one eliminates the problems of dissipative heating through shockwaves, encountered by any conventional thermometer at supersonic velocities.

In the first year of the program, Chen (1981) found that at low pressures the ratio of the speed of sound at a given frequency to the speed of sound at zero frequency changes with altitude as a result of dispersion. Consequently, for a fixed frequency signal, the speed of sound depends on the pressure as well as on the temperature, and pressure information in addition to the measured speed of sound would be necessary to obtain the correct temperature value.

Because of this and other problems in connection with the rocket launch, plans were made to defer development of a rocket launch probe.

It was decided instead to concentrate on the development of a balloon launched instrument which would only ascend to altitudes below those at which the sonic velocity ceases to be uniquely determined by the temperature. The slow motion of a balloon, together with the high rate of data acquisition would allow for studies of the small scale thermal eddy structure, of particular interest in an altitude range from the tropospause to about 30-40 kilometers.

The instrument developed measures the phase between emitted and received acoustic singals from a constant frequency source. Since the signal has propagated over a fixed distance between emission and reception it is possible in theory to determine the propagation velocity and thus the temperature of the medium of propagation. However, because of the constant phase shifts introduced in acoustic-and-electronic-components the temperature determination is to be made by means of calibration charts of temperature versus phase-shift.

The instrument consists of a constant-frequency signal-generator, a signal amplifier, a transmitter, a microphone, a bandpass filter, voltage-and phase-comparators and frequency dividers.

It was also necessary in order that the instrument withstand the environmental conditions of balloon flights from ground level to 40 km, to consider layout, insulation and mechanical operation of the flight package.

Thus, to facilitate determination of temperature from the signals produced by the electronic components, and to test the performance, reliability and repeatability of the instrument, calibration curves were obtained in AFGL's environmental test facility.

4. ACOUSTIC FLOW MEASUREMENT TECHNIQUES

It is shown in standard works on acoustics or physics (e.g. Morse & Ingard 1968) that the velocity at which small disturbances are propagated through a compressible fluid is given by the relation:

$$c^2 = (\partial p/\partial \rho)_s \qquad (1)$$

where c is the wave propagation speed, p is the static pressure, ρ the density, and s the entropy of the gas.

The temperature and velocity gradients produced in a fluid by a sound wave are so small that each fluid particle undergoes a nearly isentropic process. For purposes of computing the wave speed we assume the process to be strictly isentropic and envoke the isentropic relation for a perfect gas, $p = \text{const} \cdot \rho^{\gamma}$, where $\gamma (= Cp/Cv)$ is the ratio of the specific heats.

We also use the equation of state of an ideal gas, $pm = \rho RT$, where m is the molecular weight, R is the universal gas constant and T is the absolute temperature. This gives an expression for c which is independent of static pressure:

$$c = (\gamma RT/m)^{1/2} \qquad (2)$$

On substitution of numerical values for the constants γ, R, and m (for dry air) this equation reduces to:

$$c = 20,\ 067\ T^{1/2} \qquad (3)$$

where c is expressed in meters per second and T in degrees Kelvin.

We thus have a simple relation between the acoustic propagation velocity, and the ambient temperature.

Having derived this fundamental relationship we must examine the underlying assumptions.

The requirement that the wave is adiabatic is only satisfied if the incremental pressure due to the sound wave is very small compared to the static pressure of the medium. This condition is met in the atmosphere near the surface of the earth even with quite loud sounds. However, at heights of 25 km the sound pressure from intense sources become an appreciable fraction of the ambient pressure (19 torr ≈ 2500Pa). Therefore, if the sound impulse is transmitted at excessively high intensity the velocity becomes a function of the ambient pressure and equation (1) is no longer valid.

The signal picked up by the microphone at an ambient pressure corresponding to 25 km corresponds to only about 0.5 Pa (down from about 20 Pa at atmospheric pressure). Thus we see that the amplitude employed is small in comparison to the pressure at 25 km and that this requirement imposes no practical limitation on the present investigation.

Another assumption is made in treating γ as constant for a given gas or mixture. For waves of very high frequency a velocity dispension w.r.t. the sound frequency exists, the velocity showing an increase with frequency. An explanation for this dispersion is given by Kneser (1933). It is based upon the assumption that due to the great acceleration of the molecules produced by the high frequency sound waves, energy imparted to the molecules cannot be distributed among the various vibrational degrees of freedom in accordance to equilibrium theory.

A small but finite "relaxation time" is required for a molecule to adjust itself to a change in total energy imposed from the outside. If the sonic pressure changes act in too rapid succession, the molecule cannot achieve equilibrium. Since γ depends upon the specific heats, Cp and Cv, and these in turn depend on the energy distribution among the various translational, rotational and vibrational degrees of freedom of the molecules, it follows that γ cannot be regarded as a constant, but is a frequency-dependent variable. Barret & Soumi (1949) point out that this dispersion can be neglected when the sound frequency is less than about 500 kiloHertz.

Chen (1981) in his theoretical study on the feasibility of high altitude atmospheric temperature probes, points out that when dispersion occurs the ratio of the speed of sound at a certain frequency to the speed of sound at zero frequency depends on both pressure and temperature for a sound wave of a fixed frequency. Therefore, one would need pressure information together with the speed of sound to obtain the correct temperature.

In figure 13 of Chen's paper the speed of sound for a wide range of frequencies is seen to double between altitudes of about 65 and 90 kilometers. It should be pointed out that increasing the altitude also increases the mean free path of the molecules and thus has the same effect on the ratio of the wavelength of the sound wave to the mean free path as does increasing the frequency. Thus, the explanation of Kneser above is thought to be relevant to the behaviour of the propagation velocity found by Chen, and Chen points out that the influence of relaxation should be studied.

During the course of the investigation it was decided that developing a rocket launched instrument for studies of spatial temperature distribution in the high atmosphere (60 to 90 km) would be too difficult and lengthy as a first project goal. Therefore, efforts were concentrated on development of a balloon launched instrument for studies of the microscale thermal eddies in the mid-atmosphere (in particular from 15 to 40 km). Below 60 km the propagation speed of a signal of the frequency employed (8KHz) is equal to that at zero frequency and dispersion is therefore not considered a problem.

That the acoustic speed is not dependent on pressure at these altitudes (up to 30 km) has been verified in tests done at AFGL.

A third restriction lies in the fact that both γ and m must be considered as functions of chemical composition of a gas mixture. Atmospheric observations indicate that the composition of the atmosphere remains substantially constant up to heights well in excess of 30 km; with the exception of water vapor and carbon dioxide.

The small carbon dioxide content of the normal atmosphere may be neglected in this study. However, the water-vapor variation cannot be neglected without causing appreciable error since the speed of sound in pure water-vapor is much higher than in dry air.

It is possible to compute a correction factor based on the vapor pressure of water, on the assumption that the speed of sound may be regarded as a linear function of the relative concentration of the components of a mixture.

This is done in Appendix I where it is found that 100 percent relative humidity would cause 2°C error in a temperature measurement at 30°C, but

only 0.3°C error at 0°C. At -50°C the error is totally negligible and the effect of water vapor is therefore not considered further. This agrees with Barret & Soumi (1940) who state: "As in the case of ordinary virtual temperature, the correction becomes small at higher altitudes in the atmosphere and may be neglected above about 15000 ft." This will be particularly valid even at ground-level in the first balloon flight which is scheduled to take place in south-eastern New Mexico, an area not noted for its high humidity. However, the effect should be kept in mind during the first few thousand meters of ascent.

To measure the propagation velocity we consider a transmitter and a receiver separated by a distance d (figure 1)

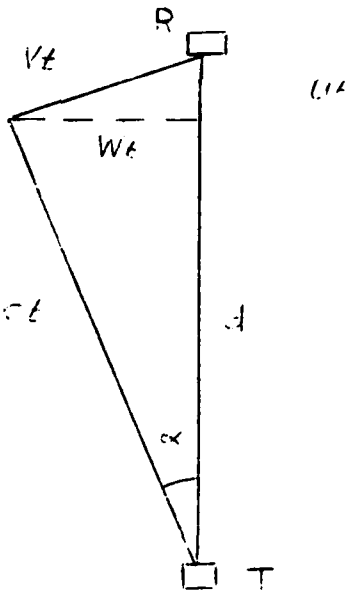

Fig. 1. Sound ray vectors showing the principle of sonic velocity measurement (adapted from Kaimal & Businger (1963)).

Assuming that the wind vector V has a component U along the sound path and a component W perpendicular to it, the transit time for a wave front traveling from T to R is

$$t = d/(c \cdot \cos\alpha + U) \tag{4}$$

where α is the deviation of the path caused by the component of the wind perpendicular to the sound path.

From equation (4) we see that the transit time is determined both by the propagation velocity and by the local wind vector in the medium.

Kaimal & Businger (1963) developed a sonic thermometer-anemometer by employing two sound waves, of different frequencies travelling in opposite directions. From the relations $V^2 = U^2 + W^2$ and $\sin\alpha = W/C$ they derive for the difference and sum of the transit times

$$t_2 + t_1 = 2dc \cos\alpha/(c^2-V^2) \tag{5}$$

$$t_2 - t_1 = 2dU/(c^2-V^2) \tag{6}$$

Equation (5) is independent of U and is and used for measuring c and thus the temperature. Knowing c, equation (6) is used to determine U.

A second method consists of adding and subtracting the reciprocal travel times, ie.

$$t_2^{-1} + t_1^{-1} = 2\,(c \cdot \cos\alpha)/d \qquad (7)$$

$$t_2^{-1} - t_1^{-1} = 2\,U/d \qquad (8)$$

Thirdly, the instrument of Larsen, Weller, and Businger (1979) uses a phase-locked loop to keep the phase difference across the soundpath constant, irrespective of wind and sound-speed variations, by varying the frequency of the sound waves.

By assuming perfect phase lock they derive the equivalent expression to (5)-(6) and (7)-(8):

$$(\omega - \omega_0)/\omega_0 + (\omega_1 - \omega_{10})/\omega_{10} = 2(c/c_0\ \cos\alpha - 1) \qquad (9)$$

$$(\omega - \omega_0)/\omega_0 - (\omega_1 - \omega_{10})/\omega_{10} = 2U/c_0 \qquad (10)$$

were $(\omega-\omega_0)$ and $(\omega_1-\omega_{10})$ are the differences between the actual transmitter frequency and the free running frequency of the phase locked loop in the two opposing directions.

Comparing these three sets of equations we observe that the phase-locked loop method has the advantage that the path length d drops out and that only measurements of relative frequency variations are necessary.

However, considered as a dynamic system a phase-locked loop, even when phase-lock is achieved, is controlled by a highly nonlinear equation. Consequently the system will become unstable if the phase difference across the feed-back becomes equal to or larger than π radians, and also whenever the transmitter frequency goes outside of the so called "lock-range" of the

phase-locked loop circuit. Prototype circuits using phase-locked loops where tried out and severe problems of stability and loss of locks were encountered. Because of the large temperature difference experienced when ascending from ground level to 25 km in the atmosphere it would have been necessary for the transmitter frequency to change from about 5 to 11 kHz if the free-running frequency of the phase-locked loop was set at 8 KHZ. Whereas this is possible, it requires that in this frequency interval the phase characteristics of the transducers must be rather flat. Larsen, Weller & Businger (1979) concludes that the only transducers fulfilling this requirement seem to be condenser microphones. These transducers, however, have a number of drawbacks, such as the need for a high bias voltage (200 V) and special preamplifers. They would also only be capable of producing sound of relatively limited amplitude, incompatible with the strong attenuation in the mid and upper-atmosphere.

For these reasons it was decided not to pursue the phase-locked loop principle but to concentrate on simple measurement of transit times from the phase difference introduced by the acoustic path. Further details on the phase-locked "closed-loop" principle can be found in Appendix V.

From the above it is noted that in the "inverse method", equations (7) and (8), U measurements are not contaminated with variations in c and W. However, since we are chiefly concerned with measurements of c, which in all three methods is contaminated by velocity fluctuations, it is not thought that going through the extra complication of trying to obtain t^{-1} would result in any major improvement of the instrument during the first few launches. Also, if required, the additional apparatus needed

to invert the measured transit times could probably be ground-based and added at a later stage.

As has been pointed out, and as can be seen from equation (5) the measured sound speed will be contaminated by the wind vector, V. This will be considered in the following chapter.

5. SONIC TEMPERATURE MEASUREMENT IN THE ATMOSPHERE

From equation (4) above the transit time for a wave to propagate from the transmitter to the receiver is given as:

$$t = d/(c \cdot \cos \alpha + U)$$

which with $\alpha = \sin^{-1} W/c$ becomes

$$t = d \{c\sqrt{1 - (w/c)^2} + U \}^{-1}$$

Thus, the transit time is seen to be dependent both on the wind velocity transverse to the soundpath, W, and along the soundpath, U; as well as on the sound speed. However, since $W/c << 1$ we can ignore the effect of W and set

$$t \approx d \{c+U\}^{-1} \qquad (11)$$

The effect of the wind velocity along the soundpath is considered in Appendix II were it is estimated that the error in temperature reading would be 0.6°C and 3°C for mean wind velocities of 5 m/s and 20 m/s respectively, with ten percent turbulent intensity.

This is a very serious error and on subsequent flights it will be necessary to add another transmitter and receiver, with soundwaves of different frequencies travelling in opposite directions, in order to eliminate the effect of the wind fluctuations, U'; as is outlined in the previous chapter.

Neglecting this velocity contamination for the first launch of the instrument we see that if the soundpath is chosen to correspond to an integral number of wavelengths at some reference temperature T_o, we have the transit time:

$$t_o = d/co = n/f \tag{12}$$

where n is chosen.

For this temperature the phase difference across the acoustic path is an integral number of 2π - i.e. zero. As the temperature changes, the resulting change in sound speed will introduce an acoustic phase difference. Thus, the transit time becomes

$$t = {}^{d}/_{c} = (n + {}^{\phi}/_{2\pi})/f \tag{13}$$

Integrated circuit phase comparators give an output voltage which is proportional to $\cos\phi$ and thus, for a single valued correspondence between this output voltage and the measured temperature, the phase difference across the acoustic path must lie between zero and 180 degrees.

Thence, the maximal and minimal sonic velocities that can be measured are given by equations (12) and (13):

$$c_{max} = c_o = d \cdot f/n$$

$$c_{min} = d \cdot f/(n+1/2) \tag{14}$$

We see that the maximum temperature range is obtained when the receiver is only one wavelength away from the transmitter. This would, however, require a very low frequency for the sound wave to travel across an air sample of meaningful size. Also, choosing n to be very small would give low sensitivity since there would be a large temperature change for little phase change.

On the other hand, if we choose a very high transmitter frequency, n will be a large number even for moderate propagation distances. This would give very good sensitivity, but a small interval of temperature over which we could measure unambigously.

Also, the attenuation of sound signals at low pressures requires that the acoustic path be limited to some ten to twelve centimeters in order for the microphone to pick up the transmitter signal at altitudes of 25 km and above. This could of course be compensated by transmitting a stronger signal, but a stronger signal would require much higher signal levels to the transmitter and be incompatible with the weight and space limitations of a balloon package.

Finally, d/e, the ratio of soundpath to transmitter diameter should not be too much smaller than one as this would put the microphone in a sound-field where the phase-change due to attenuation may not be repeatable.

Considering all these requirements, a transmitter frequency of between five and ten kilohertz was found to give both fair sensitivity and adequate temperature range.

Because the electromagnetic transmitter (see chapter 6) was found to produce a particulary strong signal for an eight kilohertz input this was chosen as transmitter frequency.

Choosing an appropriate reference temperature and using equations (3) and (14) we can calculate the measurable temperature range for given lengths of the acoustic path. This is done in Appendix III, from which we summarize four alternatives

Ref temp	Acoustic path length	Minimum temp	Temp range for a $\phi=\pi$
a) 40°C	$d = \lambda_{40} = 4.43$ cm	-134°C	174°C
b) 25°C	$d = 2\lambda_{25} = 8.66$ cm	-82°C	107°C
c) 20°C	$d = 3\lambda_{20} = 12.9$ cm	-58°C	78°C
d) 0°C	$d = 4\lambda_{0} = 16.6$ cm	-57°C	57°C

Figure 2. Temperature ranges for different choices of length of acoustic path

From the physical properties listed in Appendix IV we see that the expected temperature changes during flight will be from plus 20°C at ground level to minus 56°C at altitudes of 15 to 20 kilometers.

Thus alternatives a) and d) above have too large and too small temperature range respectively. Letting d equal to $4\lambda_0$ would also make the acoustic path too long to overcome the atmospheric attenuation.

However, choosing d equal to either $2\lambda_{25}$ or $3\lambda_{20}$ is seen to fit the expected environmental conditions well. Alternative c) would have better sensitivity but somewhat more limited temperature range than would alternative b).

In order to make practical use of the above relations and results it is necessary to (1) generate sound waves by electrical, or mechanical, means; (2) transmit the sound through the atmosphere; (3) receive the sound and convert it to electrical impulses; (4) express the time of travel of

the soundwave in terms of some electrical parameter; and (5) provide for telemetry.

The last point is done by the telemetery unit at AFGL and will only be briefly considered in Chapter 7 when performance estimates of the airborne instrument are made.

In the following chapter we consider in more detail the first four points.

6. THE BALLOONBORNE ACOUSTIC THERMOMETER (BAT)

As noted above the chosen design measures the phase shift of a constant frequency sound wave over a fixed distance, rather than measuring the frequency of a sound wave which has a fixed phase shift over a certain distance.

The flight instrument, named BAT for Balloonborne Acoustic Thermometer, employs a precision waveform generator using a crystal to control the frequency of its sinusoidal output. A linear, bi-directional power-operational-amplifier amplifies the sine-wave before it is converted into an acoustic signal by a specially developed electromagnetic transmitter. The acoustic signal is picked up, after having propagated across the air, by a sensitive condenser microphone, and filtered through a narrow active bandpass filter to remove the effect of any microphone pick-up from sources other than the transmitter. The filtered signal and a reference signal from the waveform generator are applied to voltage comparators that convert the sinewaves into squarewaves, but do not alter their phase. This is done to eliminate possible phase-errors introduced by small dc-offsets of the sinewaves. Thus we have two 8 kHz squarewaves whose phase difference is due to the passage of the signal through the acoustic medium and any phase differences introduced by acoustic and electrical components. Assuming the latter to be constant the change of phase difference between the signals should be uniquely related to the temperature of the acoustic medium.

Originally the phase shifted waves were used as inputs to a phase comparator, the output voltage at which was passed on to a voltage controlled oscillator which transformed the phase information into a

variable frequency and allowed for ease in interpretation of data using a frequency counter and calibration curves.

However, after discussion with engineers from AFGL, the circuit for the flight unit was altered slightly and the phase information presented for telemetry to ground in three different forms.

Both the filtered signal and the reference signal are delivered for telemetry after having been divided down from their original frequency by a factor of 20. This is done both as a check of the electronic circuitry and for possible application of signal processing techniques after receiving the telemetered signals on the ground. The frequency division to 500 Hz is made since no channels for telemetry are available at 8 kHz.

Both 8 kHz squarewaves are applied to an operational multiplier set up as a phase comparator with a dc-level output which varies between plus and minus π volts. Only signal levels between zero and five volts can be used for telemetry and consequently the amplitude of the dc-signal is reduced by one third in an attenuator and 2.5 volts added to it in a summing amplifier before it is delivered.

Finally, a digital phase counter* uses flip-flops, a binary counter, latches, digital gates and a high frequency clock to produce a digital signal proportional to the phase shift. By using a 4 MHz crystal as clock and letting the zero crossings of the two phase shifted signals determine whether the counter is enabled or disabled this circuit gives 500 digial counts for 360 degrees of phase shift.

A block diagram of this set up can be found in figure 3.

* This was developed by Gautham Ramohalli.

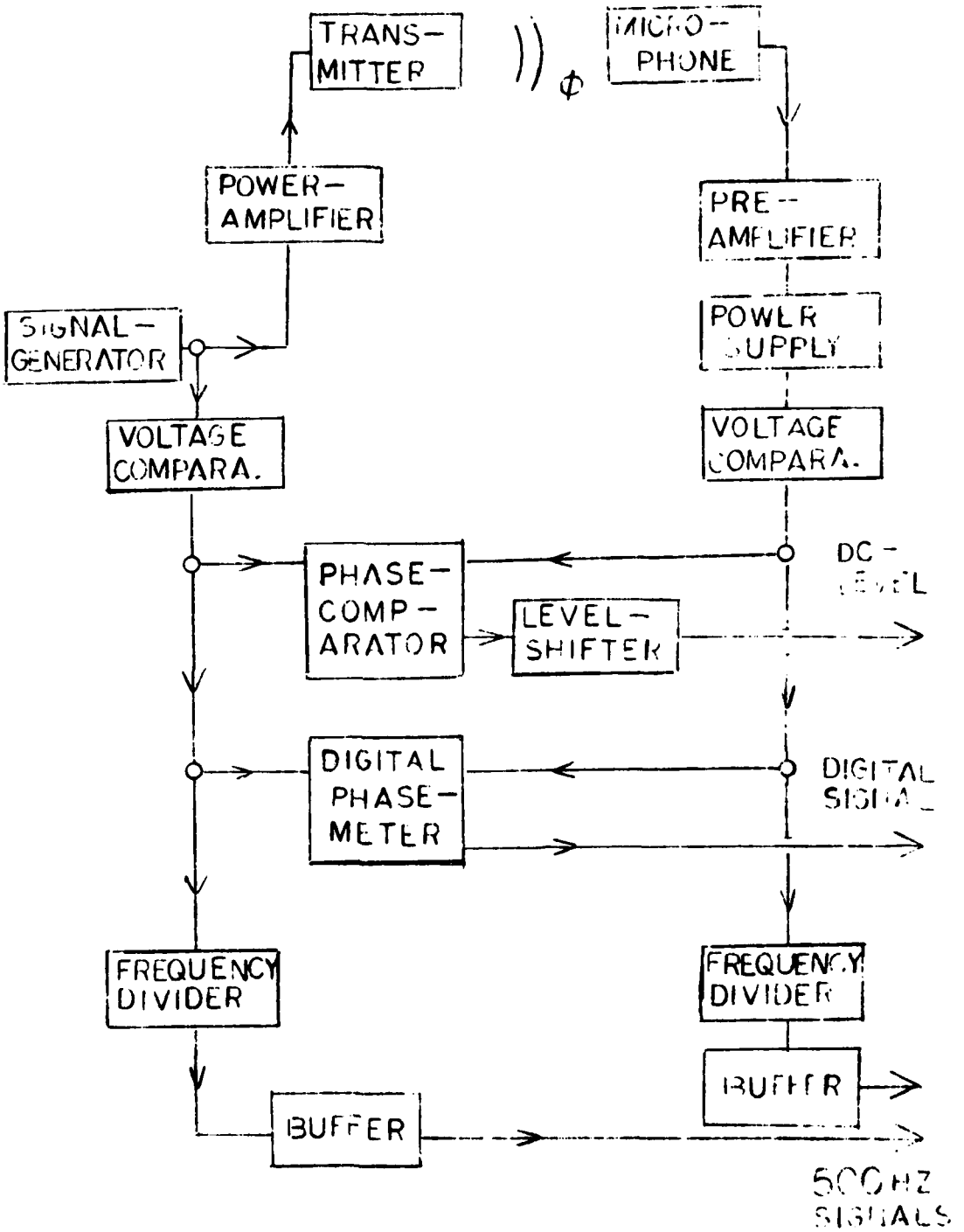

Figure 3. Block diagram of the Balloonborne Acoustic Thermometer (BAT)

The route leading to the final design was by no means straightforward and a variety of set ups, using partly different circuit components have been tried.

A description of a "closed loop" feedback system using a phase locked loop integrated circuit is given in Appendix V. This set-up is similar to the one of Larsen, Weller and Businger (1979), mentioned previously.

Further details on the evolution of tne final instrument are not thought to be essential and are not included. The interested reader is refered to internal memos AR 1042, AR 1044 and AR 1045 of M.I.T.'s Aerophysics Laboratory as well as to the quarterly progress reports furnished by the Aerophysics Laboratory to AFGL.

Below is given a fairly brief description of the individual components. For a more detailed description with circuit diagrams and specifications, refer to Apendices VI and VII, or to the "user-manual" supplied to AFGL with the finished instrument.

THE ELECTRONIC COMPONENTS

The electronic circuitry, apart from the power operational amplifier and relays, is placed on five 4x4" pc-boards which are connected to a common 50 strip bus line by cartridge connectors. Because of the large changes in ambient temperature during a balloon flight, and to ensure precision and reliability, high grade electronic components have been used wherever possible.

For pictures of the circuit boards see figures 4 and 5.

The Generator board

This circuit board consists of an XR 8038M precision waveform generator, set up to produce a low distortion sinewave. To ensure minimal

frequency drift the waveform generator is crystal controlled. Thus a 8 kHz quartz crystal is set up to act as a parallel resonant device. This crystal has an equivalent capacitance of 6 to 9 picoFarad. The generator will free-run, without the crystal installed, at approximately 9.8 kHz and will lock in on the quartz crystal which will then act as the primary frequency control element.

Typical specifications for the generator board are:

Generator frequency: f_p = 8000 Hz

Frequency calibration: ± 0.003% at +25°C
(equivalent to ± 0.24 Hz at 8000 Hz)

Drift with temperature: Parabolic curve centered at 25°C, with negative temperature coefficient above and below this temperature. Typically for $-25°C \leq T \leq 50°C$: $\Delta f_p = \pm 0.005\%$.

Temperature range of operation of electronic components:
-55°C, +125°C.

Distortion level of signal output THD ≈ 0.5%.

The sinusoidal output signal is buffered using an operational amplifier to eliminate unwanted feedback effects from other circuit components. The output is passed on to the power amplifier and is also used as the reference signal for phase measurement.

For more complete technical specifications and a circuit diagram of the generator board see Appendix VI.

The power amplifier

The sinusoidal signal from the generator board is amplified by a Torque Systems PA 112 linear bidirectional power op-amp to about 15 Watts before being applied to the electromagnetic transmitter.

Operating temperature range of power amplifier: 0°C to 50°C.

The filter board

To remove any effect on the measured phase difference of acoustic signals from sources other than the transmitter it was thought necessary to pass the microphone signal through an extremely narrow bandpass filter, centered at the transmitter frequency.

The filter chosen is a 2 pole (4th order) state-variable active bandpass filter based on a general design given in "the Active Filter Cookbook" by Lancaster (1975).

The filter consists of six high class operational amplifiers, LM 101, and has the following characteristics.

Center frequency: f_e = 8000 Hz

Amplification ratio for each stage (pole): $Q_1 = Q_2 = 100.$

Staggering value for maximum flatness in response: a = 1.005

Staggered filter response e_{out}/e_{in} = 59 dB - 7 dB (insertion loss)

= 398.

Temperature range of electronic components -55°C, +125°C.

To avoid any interference by the filter on the microphone the microphone signal is buffered before the filter input. After this buffer the microphone signal is attenuated to avoid saturation due to the high amplification ratio of the filter. The sinusoidal filter output is passed on to a voltage comparator for transformation to a square wave.

A more detailed account of the filter board is given in Appendix VI.

The comparator board

Both the filtered microphone signal and the reference signal are passed on to this board where they are converted from sinewaves to squarewaves by two LM 111 voltage comparators. This is done because voltage comparators operate at saturation and thus will produce constant amplitude outputs (5 Volts), as long as the input amplitude is larger than some threshold value (~4 mV). Hence, the voltage comparator outputs are independent of the changing attenuation of the acoustic signal as the balloon ascends and descends.

Also, if the microphone signal is small, any offset voltage, even if very small, may alter its phase information. This will not be the case, however, for the square-wave signal unless the offset is larger than half its signal amplitude.

The phase information is extracted and presented for telemetry by three different methods:

(1) Using two LM 14040B 16 stage binary counters, the 8 kHz signals are changed to 500 Hz for telemetry. This was necessary to make the signals compatible with available channels in the telemetry unit.

In dividing down the signal frequencies by a factor of 16 we also reduce the phase shift between the signals by the same factor. Thus instead of a maximum phaseshift of 180 degrees we get only 11.25°.

However, the time-difference between the cycles is still the same (a 500 Hz cycle is 16 times as long as an 8 kHz cycle!) and hence, if the signals can be treated by timebased signal processing techniques, no loss of resolution should result.

By tying the 250 Hz ouptut of the "reference-counter" to the enable input of the "phase shifted-counter" the waveform of the phase-shifted signal is modulated by the phase shift. This makes recording of the data easier. In order to be able to calibrate out any phase shift introduced in the telemetry equipment it was necessary to provide a possibility for looking at the same signal on both telemetry channels simultaneously. This is done by a switching relay, set up such that whenever a "command on" pulse is applied to the instrument the reference signal will also be on the channel which otherwise holds the phase shifted signal.

(2) Further, the 8 kHz signals are passed on as the inputs to an XR 2208M four quadrant multiplier, set up as a phase comparator.

The differential dc voltage, V_ϕ, at the two multiplier outputs is related to the phase difference between the two input signals as:

$$V_\phi = K_d \cos \phi \tag{15}$$

where K_d is the phase detector conversion gain. For input signals above 50 mV, K_d is given by Exar as approximately 2 V/radian and is independent of signal amplitude. Thus the phase comparator will vary from 3.14 volts, at ϕ equals zero degrees, to -3.14 volts, at ϕ equals 180 degrees.

However, since only signal levels between zero and five volts are acceptable for telemetry, the signal is passed through a difference

amplifier, an attenuator and a summing amplifier where +2.5 volts dc is added.

Both V_ϕ and the two 500 Hz signals are buffered before being delivered to the telemetry unit.

Temperature range of electronic components: -55°C to 125°C

For specifications and circuit diagrams of the comparator board see Appendix VI.

The digital board

(3) A digital phase counter, developed by Gautham Ramohalli*, has been incorporated into the design. This circuit uses Motorola CMOS digital logic circuitry and a 4 megaHertz crystal as a clock to count the number of clockpulses between the cycles of the two 8 kiloHertz squarewaves from the voltage comparators described above.

The 8 kHz signals are applied to dual type flip flops which enable and disable a binary counter. Thus, when the first square wave goes high the counter starts counting clockpulses. When the second squarewave goes high the counter is disabled and thus information about the phase between the two waves now exists in the counter in the form of a digital number of clockpulses counted. This 8 bit digital number is then latched into three dual latches if enabled by a master sampler. The master sampler is derived from the clock through a 24-stage frequency divider and can be changed for

*Now with Honeywell Inc., Minneapolis, MN.

compatibility with the telemetry equipment. It is presently set at one Hertz, the expected transfer rate of the digital signal to ground.

After opening the latch gates the circuit waits two clock pulses to ensure that the data have been latched in. Then the gates are closed so that the data will not change as the counter is reset. Two more clock-pulses are counted to make sure that the gates are closed, whereupon the counter is reset and the cycle starts again.

It should be noted that this digital counter is capable of delivering digital phase information at rates approaching 8 kHz if the master sampler is changed appropriately, and also that it operates over 360 degrees of phase shift.

The digital circuit components used include MC 14011B NAND-gates, MC 14013 Dual type flip flops, an MC 14040B Binary Counter, MC 14042B Quad latches, MC 14049B Hex buffers and an MC 14521B 24 stage frequency divider.

The temperature range for these components: -40°C to +75°C.

For more information, specifications and a circuit diagram of the digital board, see Appendix VI.

The regulator board

The circuitry described above operates between ± 12 Volts with the following exceptions:

- the power amplifier requires ± 24 V;
- the voltage comparators and binary counters are set up to work between +5 Volts and ground to make the level of the 500 Hz signals compatible with telemetry requirements;
- all digital circuitry works off + 5 Volts.

The airborne power supply will be 23 times 1.5 Volt batteries, initially delivering ± 34.5 Volts. This is regulated down to ± 24 Volts, ± 12 Volts and + 5 Volts, using Motorola voltage regulators of the MC 78- and MC 79-series. The use of voltage regulators ensures a constant supply voltage as the batteries use up part of their charge throughout the flight.

The power requirements for the electronic circuitry is only some one hundred milliAmperes at most. The power amplifier delivers about 15 Watts at ± 24 Volts to the transmitter. From specifications about power dissipation at max supply (60 Watts) the amplifier should draw well under 24 Watts, which would be equivalent to 1 Ampere.

The voltage regulators are rated for 1.5 Amperes continuous supply but because of the harsh environment, and to minimize the possibility of power-failure, the regulators were set up for much less than full load. Thus two pairs of regulators are set up in parallel to supply plus and minus 24 Volts to the amplifier only. The outputs of these regulators are connected by diodes to avoid current flow between them due to small differences in the regulated voltage.

To supply the electronic components the plus and minus 24 Volt regulators are powering ± 12 Volt regulators, the + 12 Volt regulator supplying a + 5 Volt regulator.

The voltage regulators have been tested at AFGL in temperatures down to -60°C. When turned off and allowed to cool down to ambient temperature, they required some 20 seconds before regulating the correct voltage level when turned on again.

For specifications and circuit diagram of the regulator board see Appendix VI.

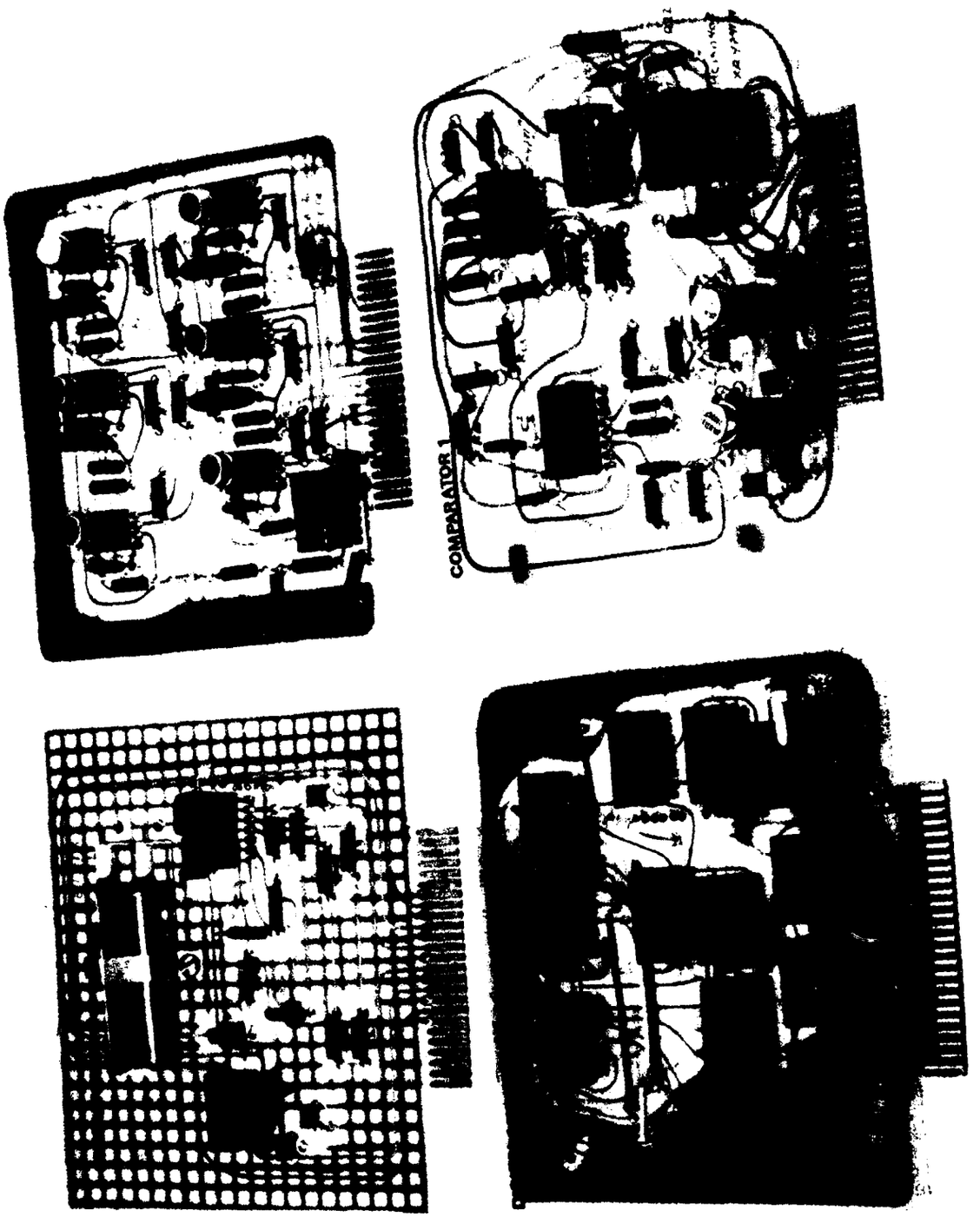

Figure 4. Component side of the electronic circuit boards

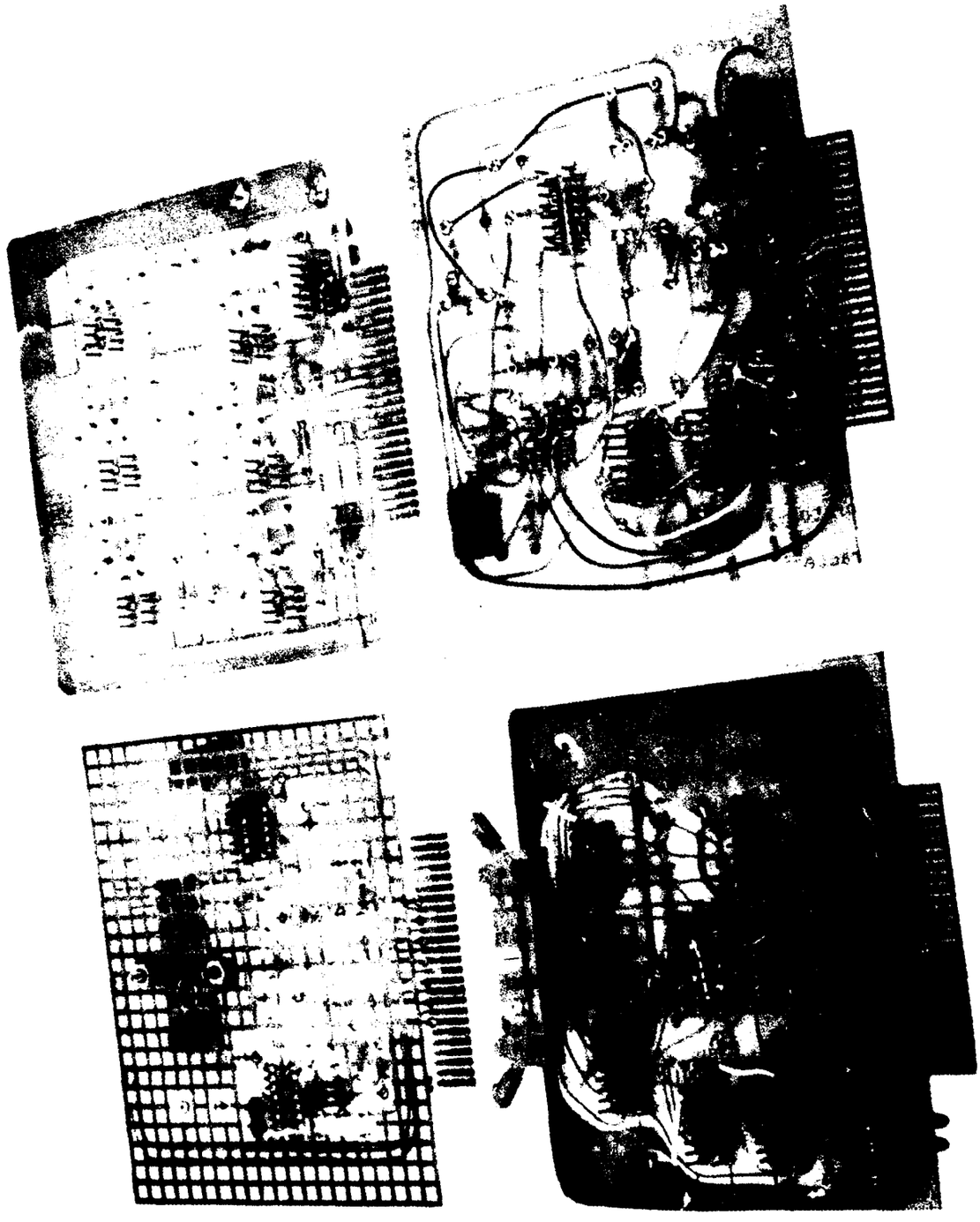

Figure 5. Reverse side of the electronic circuit boards

THE ACOUSTIC COMPONENTS

To overcome the severe attenuation experienced during ascent through the atmosphere a transmitter capable of producing a fairly intense acoustic signal is required.

In the first year of this program an electrostatic transmitter was developed and shown to be capable of producing the necessary signal amplitude for use up to 90 km of altitude (see Chen (1981)). However, repeated problems with arcing across the aluminized Mylar film rendered this transmitter far too unreliable for airborne testing purposes.

Commercially available speakers of type JBL 2105 were tried and found to give the required amplitude. But during tests in the Aerophysics laboratory they were found to have inconsistent and unrepeatable phase characteristics. Thus, the phase difference measured when cooling the acoustic path, and transmitter, down was not the same as that measured at the same air temperature when letting the medium warm up.

It is believed that this is because these speakers employ viscous suspension of the transmitter cone to its casing. The viscosity of the suspending substance would most probably change with temperature, with a delay relative to the ambient temperature, and this would explain the observed change in phase characteristics. However, the change of viscosity is likely to be dependent on localized temperature variations across the transmitter surface due to both the rate of cooling of the medium and the power dissipation, thus accounting for the unrepeatability.

Consequently it was necessary to develop and test an alternative transmitter.

The electromagnetic transmitter

The designed transmitter relies on electromagnetically induced vibrations for its sound production. An aluminumized-Mylar laminated film has been etched such that only a conducting spiral pattern remains on the Mylar surface. This diaphragm is suspended in the fringing radial field of a Samarium-Cobolt permanent magnet disc.

The magnetic disc is centered inside an aluminum drum and mounted to the top of an adjustable screw which is attached through the back-surface of the drum casing. Thus the distance between the magnet and the mylar membrane is adjustable, since the membrane is stretched tightly over the top of the drum by an aluminum ring. The attachment method being totally independent of any viscous suspension is thought to be of great importance, as mentioned above.

The spiral pattern membranes were constructed at AFGL by sensitizing, photographically exposing, developing and etching aluminized mylar film of total thickness two thousandths of an inch.

The amplified sine signal from the power amplifier is passed on through the magnet support screw and the magnet and then through the conducting spiral to ground potential in the drum casing. Since an alternating current is passing through a magnetic field that has a component at right angles to the conductor the resulting electromagnetic force causes the mylar film to vibrate at the frequency of the ac-signal.

The transmitter proved to have a highly frequency-dependent amplitude response. This, however, is not a major concern since the present instrument employs a constant frequency transmitter signal. The output characteristics of the speaker were nearly independent of membrane tension. The

distance of the magnet from the membrane had a somewhat stronger effect on the output and a spacing of some one fifth of an inch was found to give the largest amplitude.

Furthermore, the position of the magnet strongly changes the phase characteristics of the transmitter. This is to be expected since moving the magnet will change the ratio of the radial component to the axial component of the magnetic field which pass through the diaphragm. Since the radial component induces axial vibrations and the axial component seeks to induce radial components the deflection mode of the diaphragm will change, thus altering the phase characteristics.

Typical performance of the electromagnetic transmitter, when tuned for 8000 Hz, which turned out to be one of many "resonant peaks", was found to be 2 Volts of signal picked up by the condenser microphone at atmospheric pressure when a 10 Volt signal (15 Watts) was applied to the transmitter and the sound path was some 10 cms long. This gives a -14 dB fall off due to the transmitter, the microphone and the acoustic path.

At the lowest pressure tested, 10 mbar, corresponding to some 31 kms of altitude, the falloff ratio was -54 dB. This is equivalent to a microphone signal of 21 mV, which when applied to the filter input gave some 0.2 V filter output and resulted in proper operation of the phase measuring part of the circuit.

The transmitter was cooled down while operating at AFGL in order to test its ability to withstand the expected environmental conditions. At an air temperature of -60°C the transmitter was shut off and the diaphragm allowed to cool down to air temperature. When reapplying the amplifier signal the transmitter was found to consistently resume operation.

For specifications on the transmitter see Appendix VII.

The condenser microphone

To pick up the acoustic signal, which may be strongly attenuated from passing through a low density medium, use of a microphone of very high sensitivity is necessary.

The microphone used, a Bruel & Kjaer Type 4165 condenser microphone with a half inch diameter cartridge, has a sensitivity of 50 millivolts per Pascal pressure change. With the microphone signals mentioned above this corresponds to ratios of sound pressure to sea level atmospheric pressure and 30 km atmospheric pressure of 4.10^{-4} and 3.10^{-4} respectively. Thus, the requirement of low sound pressure relative to ambient pressure, examined in the theoretical analysis, is met.

The microphone is attached to a Bruel & Kjaer Type 2619, half inch preamplifier. The microphone cartridge needs 200 Volts dc polarizatrion voltage on one side of its diaphragm for operation. This, as well as 28 Volts dc needed to power the preamplifier, is supplied by a B&K Type 2804 Microphone power supply which in turn is powered by three 1.5 Volt alkaline batteries. Ths power supply is capable of driving two microphone/preamplifier units for 40 hours before change of batteries is necessary.

The microphone power supply also serves as an adapter for passing the microphone signal from B&K's microphone cable and plugs onto a Bnc connector.

Some important characteristics of the microphone, pre-amp and supply are:

Microphone, B&K 4165 --
Open circuit sensitivity 50 mV/Pa
Temperature coefficient
(between -50°C and +60°C) 0.0012 $^{dB}/_{°C}$ (~100 ppm)

Influence of realtive humidity <0.1 dB
(in absence of condensation)

Preamplifier, B&K 2619 --
Maximum sinusoidal output voltage 4V rms

Power supply, B&K 2804 --
Signal attenuation 0 dB
Temperature range 0°C to 40°C.

The microphone and preamplifier were tested and found to operate normally down to temperatures of -60°C.

For more detailed specifications of these components see Appendix VII.

For pictures of the electromagnetic transmitter and condenser microphone with its preamplifier attached, see figure 6.

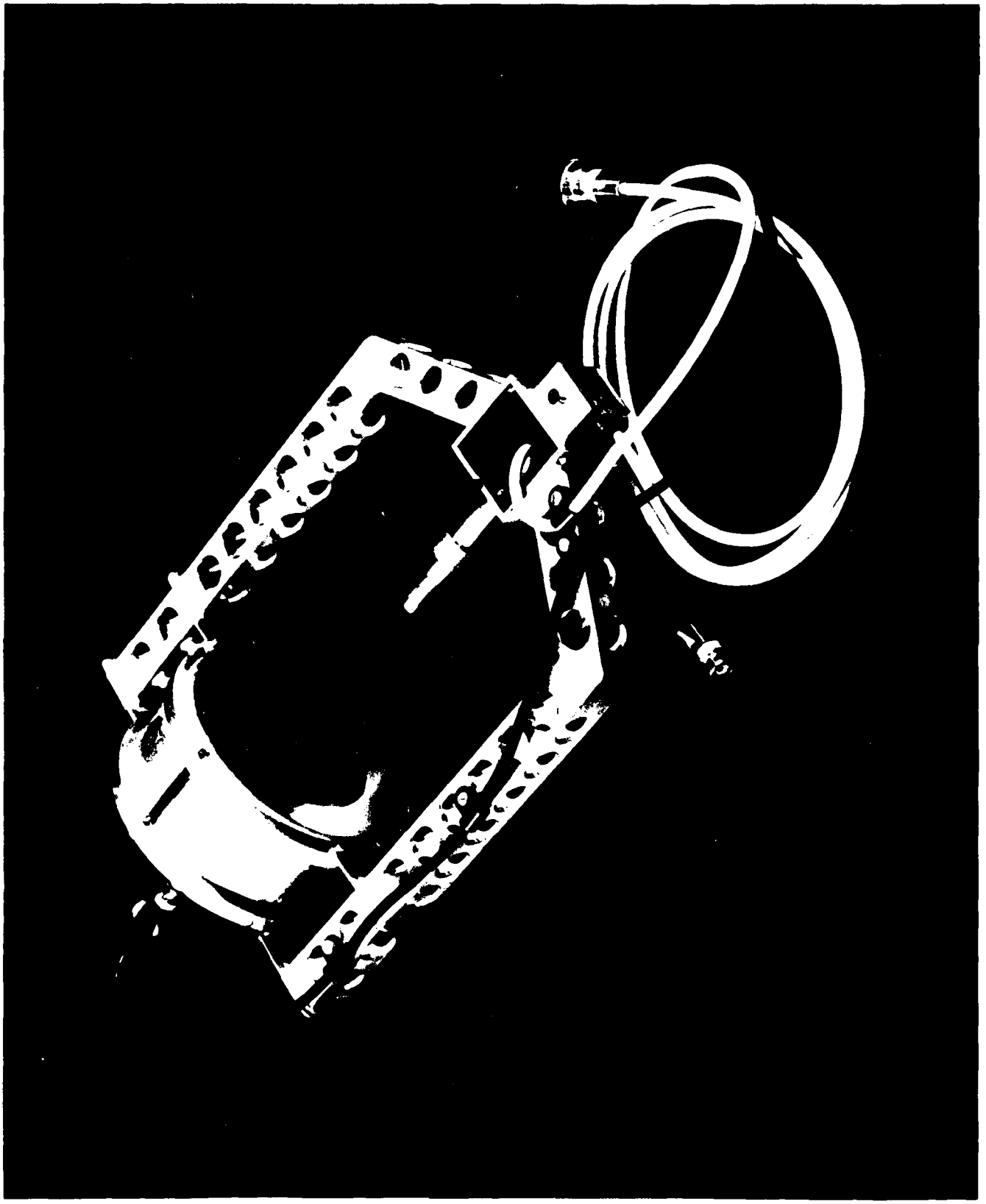

Figure 6. Front view of the electromagnetic transmitter and condenser microphone

THE CASING AND INSULATION

The electronic components described above plus the power supply for the condenser microphone are contained in a 17x15x6" aluminum chassis box with a removable aluminum top surface. A hinged lid is placed in the top surface and this lid opens to allow easy access to the circuitry. For ease of transportation the chassis box is equipped with a removable carrying-handle.

The five circuit boards are inserted in Scotchflex cartridge connectors that are tied together with a 50 line bus strip. This allows easy interconnection of the boards, which can be removed from the chassis box individually for maintenance and troubleshooting. The multistrip is attached in the middle of the chassis box floor with the microphone power supply and power amplifier on each side.

One of the "end walls" of the box hold all the electrical connections. Thus, plus and minus 30 Volts supply voltage and ground are received through three Bnc connectors. Seven additional Bnc connectors deliver and receive various signals for connection with the acoustic components, telemetry and for troubleshooting. They are, the power amplifier signal to the transmitter; the filter input to the bus strip from the microphone supply; the dc voltage from the phase comparator and the two 500 Hz signals for telemetry; and the oscillator-and filter outputs for troubleshooting.

Also, a 4 foot multistrand cable with a 26 pin Bendix connector is passed out of the chassis box to the telemetry unit. This cable and Bendix plug holds the eight bit digital signal for telemetry; connections for the "on" and "off" commands for the power supply of the flight instrument; and two free connections that can be used to obtain information about, and monitor, the temperature in the chassis box. The "on" and "off" commands

are applied to a latching relay which is connected up in parallel with the switching relay described in the section on the comparator board.

For pictures of the chassis box with the electronic circuitry installed, see figures 7, 8 and 9.

For more details on the flight instrument, with wiring diagrams and scale drawings, refer to the Instruction Manual for "Ballonborne Acoustic Thermometer," to be delivered with the instrument to AFGL.

The question on whether and how much insulation will be needed is far more complex than it might seem at first sight.

The instrument, on ascent to altitudes of 25 kms will be exposed to temperatures ranging from ground temperature (~20°C) down to about -56°C. The transmitter and receiver have been tested and found to operate satisfactorily in this temperature range. This is also the case for the voltage regulators.

Most of the electronic components are of milspec rating with operating temperature ranges down to -55°C. However, the PA 112 power amplifier and the B&K 2804 power supply are only rated down to 0°C.

It is important to remember that because of radiative heating in the atmosphere, the temperature of the gondola of the balloon and of the instruments attached to it will not be the same as the temperature of the surrounding air. Experience from previous balloon flights of AFGL indicate that the temperature in the gondola can be as much as 60 to 70°C above ambient in flights to about twenty kilometers altitude. Thus it is feared that power dissipation may cause certain of the electronic components, in particular the voltage regulators, to overheat and malfunction if the flight instrument is insulated too thoroughly.

Calculation of the expected heat transfer and temperatures across the walls of the chassis box was attempted by following the methods described by Lichfield & Carlson (1967). This analysis can be found in Appendix VIII. However, their procedure involve far too many "guesstimates" of factors like "percentage of flight package being exposed to sunlight" to give any meaningful answer.

Correspondingly it is believed that the only possible method of dealing with the question of insulation lies in actually trying the instrument out in the atmosphere. The electronic components have been moderately insulated by surrounding them with foam. (As can be seen in figure 9; note in particular the complete enclosure of the microphone power supply.)

If necessary it is possible to wrap the chassis box and surrounding gondola with aluminized mylar as a radiation shield, and /or heat the non-milspec electronic components using the excess heat from the voltage regulators.

Both the attachment of the chassis box to the gondola and the support boom for positioning the transmitter and microphone some distance away from the gondola have been designed by Richard Borgesen at AFGL.

The mounting for the chassis box is to be by means of screw-rivets to a mounting bracket.

The transmitter and receiver are to be held rigidly with respect to one another in a craddle which thus ensures that the acoustic path is of constant length. It will however be possible to adjust the length of the acoustic path to compensate for any constant phase shift in the acoustic- and electronic-components.

The craddle holding the acoustic instrumentation will be positioned about four feet from the gondola at the end of a telescopic retractable arm. The balloon will take off with the arm extended but on coming down to land the telemetry command to deploy the parachute will cause a "constant-torque" spring to retract the arm and pull the craddle inside of the gondola. (See figure 7 for a picture.)

More details on these components will be found in the instruction manual for the instrument.

The weight of the chassis box and electronic components is some 10 to 12 pounds, whilst the transmitter and microphone weigh less than 5 pounds.

Thus, the total weight of the experimental equipment, including the craddle, chassis box mounting and retractable arm, as well as batteries for the ± 35 volts power supply, is estimated to be well under 75 pounds.

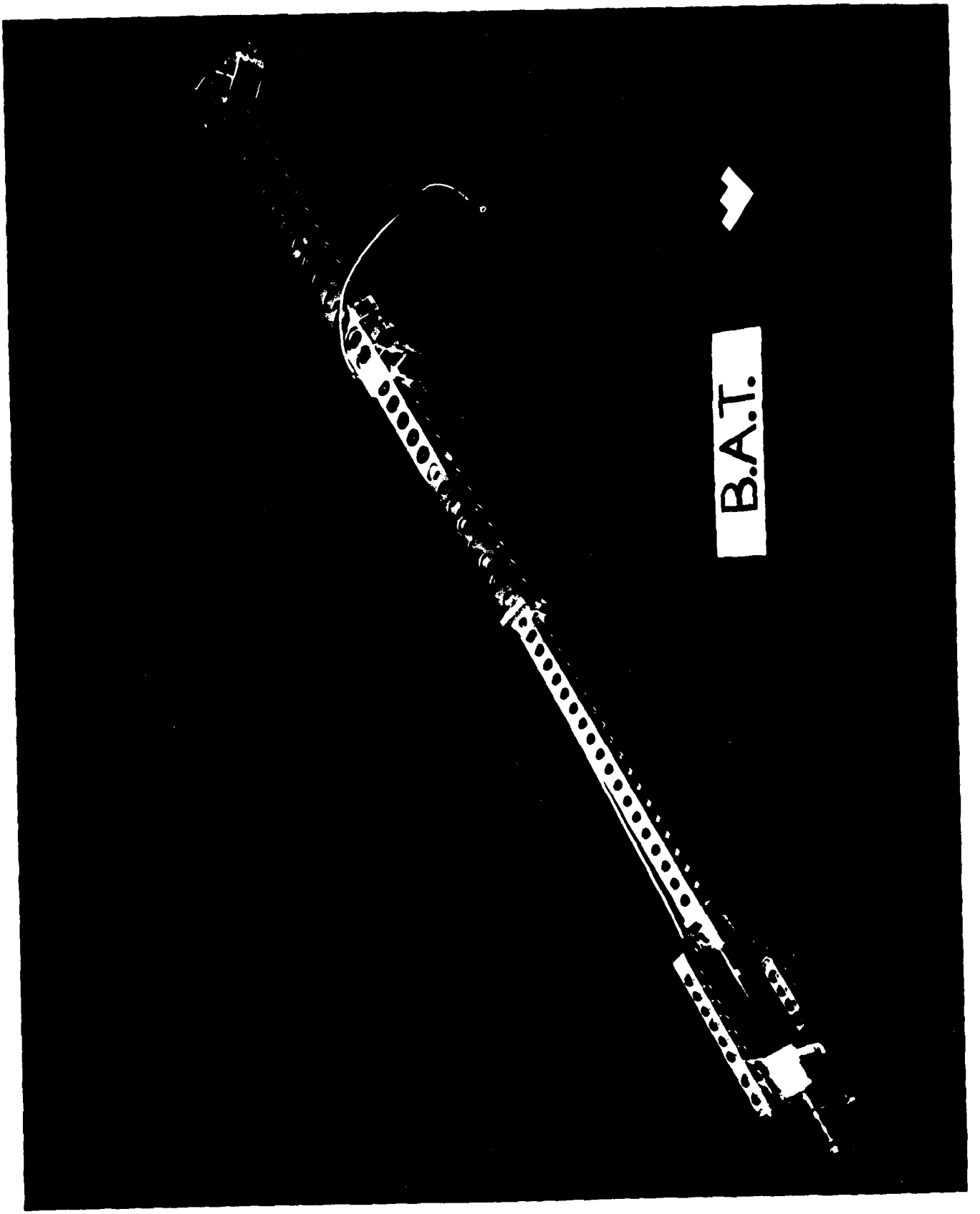

Figure 7. The arm for holding the acoustic components

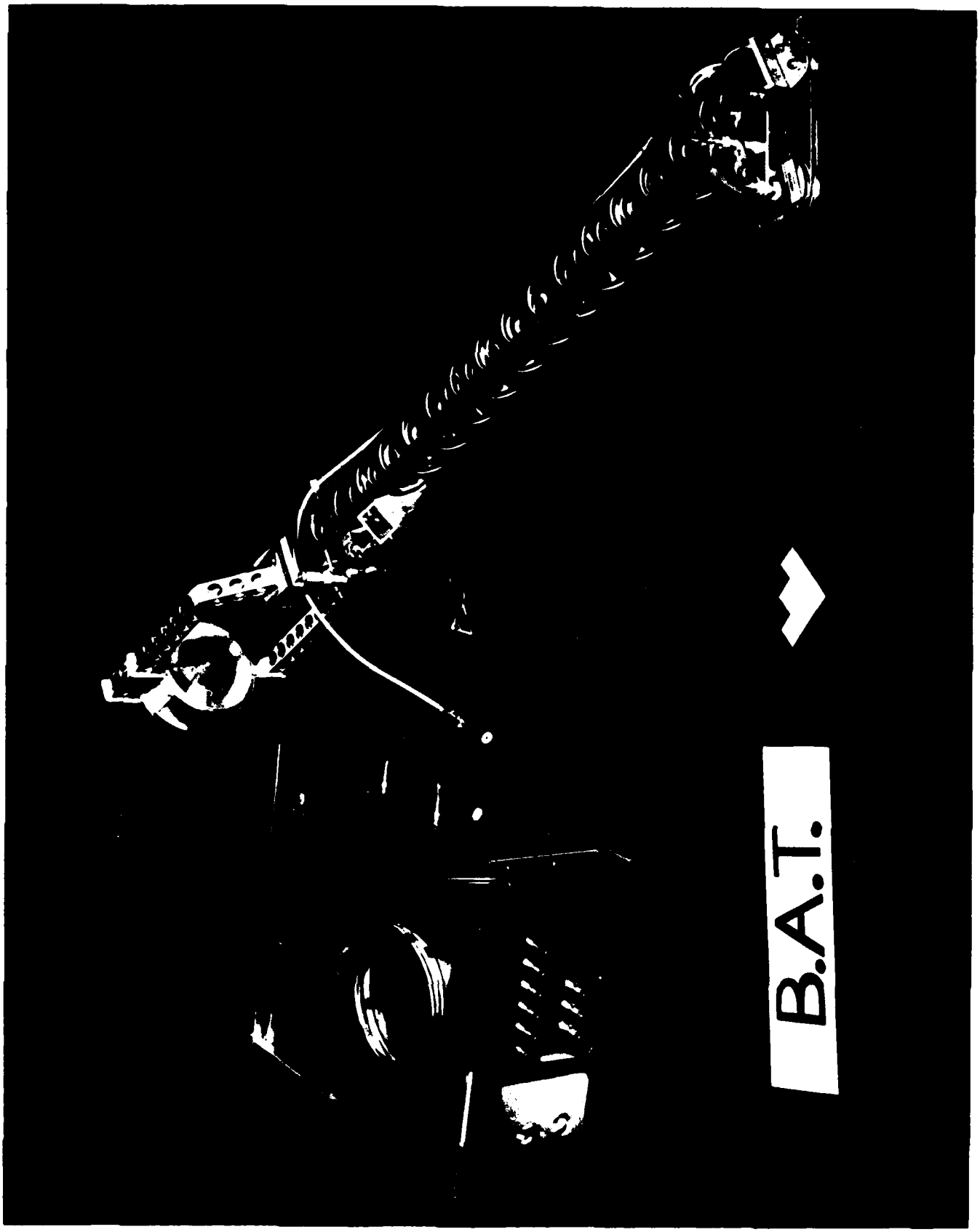

Figure 8. Exterior view of the flight instrument

Figure 9. Interior view of the flight instrument

7. TEMPERATURE MEASUREMENT

We now calculate the expected sensitivity of the three telemetry signals containing the air-temperature information.

The dc voltage from the phase comparator varies between zero and five volts. Taking 10 mV as a representative number for the smallest meaningful voltage change (this is also suggested as a typical value of the noise level in telemetry) we get as a rough estimate of the sensitivity for the different acoustic paths considered in chapter 5.

	x	ΔT_{total}	$\Delta V/°C$	ΔT_{Min} for ΔV
b)	$2\lambda_{25}$	107°C	47 mV	1/5 °C 9.3 mV
c)	$3\lambda_{20}$	78°C	64 mV	1/6 °C 10.7 mV
d)	$4\lambda_{0}$	57°C	87 mV	1/8 °C 10.9 mV

Fig. 10 The expected sensitivity of the phase comparator output

The digital phasemeter uses a 4 MHz clock to count the phaseshift between two 8 kHz signals and thus produces 500 counts for a phase shift of one full cycle. Consequently we have 250 digital bits for 180° of phase shift which results in the following sensitivities.

	x	bit/°C	°C/bit
a)	$2\lambda_{25}$	2.3	0.43
b)	$3\lambda_{20}$	3.2	0.31
c)	$4\lambda_{0}$	4.4	0.23

Figure 11. The expected sensitivity of the digital phase meter output

For the modulated 500 Hz signal the full scale difference corresponding to 180° of phase shift between the 8 kHz signals will give 11.25° of phase shift. This corresponds to 0.1°, 0.15° and 0.2° of phase shift per degree centigrade of temperature change for alternatives b), c) and d), respectively.

Had the instrument been ground based these sensitivities could have been realised with rates of data aquisition of 8000 times per second. However, in the telemetry process some of the sensitivity and much of the rapidity is lost.

Thus the phase comparator voltage can only be telemetered twice per second and with a maximum accuracy of about 0.2 °C. The digital signal will only be available once every second with the sensitivity halved due to telemetry. The 500 Hz signals, however, can be telemetered continuously.

Since the limiting sensitivity of the signal which has the highest resolution, the phase comparator signal, is set by telemetry we see from figure 10 that the obvious choice of acoustic path is b). This choice gives the largest temperature range, in case anomalous atmospheric conditions are encountered and also has the shorter acoustic path, giving the least attenuation of the acoustic signal.

This choice gives the following specifications for the instrument:

Length of acoustic path	$x = 2\lambda_{25} = 8.7$ cm (3.41")
Phase comparator signal	Twice per second with 0.2°C accuracy
Digital phasemeter signal	Once per second with 0.8°C accuracy
Continuous wave signal	Continuous with unknown accuracy (would depend on method of data treatment)

Figure 12. The expected behavior of the final design

In the previous estimate of the response we assumed that all signals vary linearly with temperature over the complete temperature range. However, this is not an exact assumption since the temperature is proportional to the square of the sound speed. Moreover, the most sensitive signal, the phase comparator output voltage, changes as the cosine of the temperature induced phase change.

To indicate that this does not seriously affect the above assumptions we present below the derivation of the exact response of the dc-level telemetry signal from the phase comparator for a one-dimensional source.

Denote

T	temperature
c	soundspeed
λ	wavelength
d	acoustic path length
f	frequency
ϕ_A	phase difference across the acoustic path
ϕ_c	phase difference across the acoustic and electronic components
$\phi_T=\phi_A+\phi_c$	total phase difference as seen by the phase comparator

Let subscript zero denote reference conditions

At To:

Initially set the acoustic path length $d = 2\lambda_0$

The resulting output of the phase compactor $\phi_T = \phi_c$

Increase the acoustic path by a distance x such that $\phi_T = 0$

Thence, we can write the acoustic path as -

$$d = 2\lambda_o + x$$
$$= ((4\pi + \phi_c)/2\pi)\ \lambda_o \qquad (16)$$

At some general temperature T, the phase comparator will see

$$\phi_T = \phi_A + \phi_c$$

and thus the acoustic path length can be written as

$$d = 2\lambda + x + \frac{\phi_A}{2\pi}\lambda \qquad (17)$$
$$= \frac{4\pi + \phi_c + \phi_A}{2\pi}\lambda$$

Equating (16) and (17) and writing ϕ_c as $\left(\frac{d-2\lambda_o}{\lambda_o}\right) 2\pi$ we get upon rearranging -

$$\phi_A = 2\pi\ (d/\lambda_o)\ \{\lambda o/\lambda - 1\} \qquad (18)$$

We now use equation (15) for the phase comparator voltage and $\lambda_0/\lambda = c_o/c = (T_o/T)^{1/2}$, to get

$$V_\phi = K_d \cos\{2\pi\{(d/\lambda_o)[(T_o/T)^{1/2} - 1)\}\} \qquad (19)$$

The manufacturer, Exar Inc., gives the phase comparator conversion gain of their XR 2208 integrated circuit component as "roughly 2V/rad." It has been found however, during testing of the circuitry, that 3.7 Volts is the

exact value. Thus, the equation for determining the attenuated, dc-shifted telemetry signal as a function of the ambient temperature becomes

$$V_s = \left(\frac{2.5}{3.7}V_\lambda + 2.5\right)$$

$$= 2.5\left[1 + \cos\left(2\pi\left\{\left(d/\lambda_0\right)\left(\left(T_0/T\right)^{1/2} - 1\right)\right\}\right)\right] \qquad (20)$$

Equation (20) is plotted as V_s vs. T for T_0 = 25°C in figure 13 where it can be seen that it approximates closely the following straight line segments

Temperature range	Slope	ΔT min
-65°C to -15°C	70 mV/°c	1/7°C
-15°C to 5°C	38 mV/°c	1/4°C
5°C to 25°C	14mV/°c	1°C

Thus we see that over most of the expected temperature range (above an altitude of about 5 km), the one-dimensional theory predicts that the telemetry equipment will set the limit to the attainable sensitivity.

Having chosen a final design we go on now to consider the environmental testing and calibration of the finished instrument, the problems encountered, and their subsequent solution.

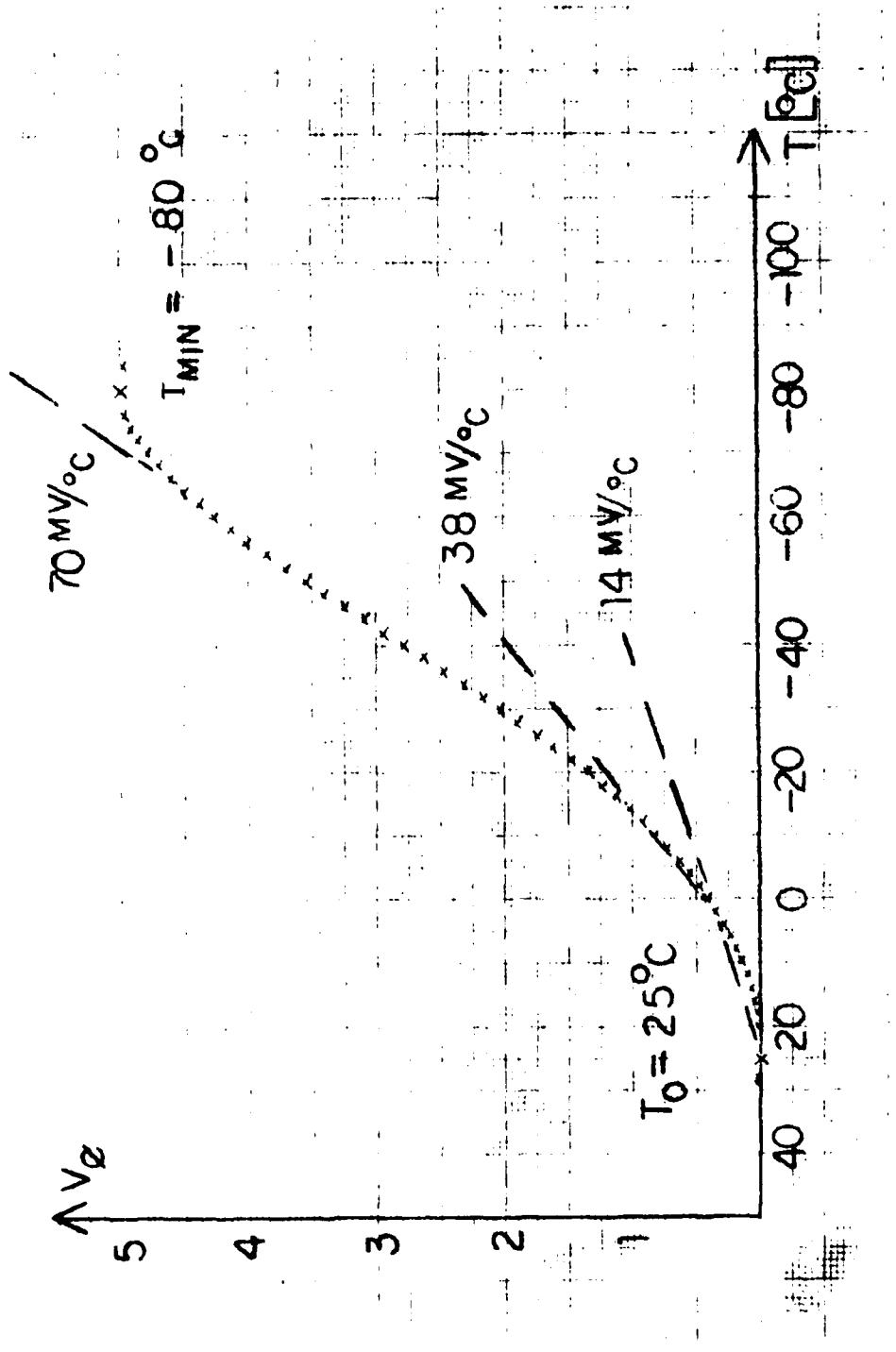

Figure 13. The one-dimensional theoretical response of the dc-telemetry signal.

The environmental testing and calibration of the instrument took place in AFGL's low-pressure chamber. This chamber allows for temperature control by cooling the chamber walls with liquid nitrogen. The flow of nitrogen, through channels in the walls, is controlled by an adjustable thermostat. Thus it was believed that the environmental conditions encountered in flight could be closely modelled.

The acoustic components were tested in the chamber with the necessary electrical signals fed in through connections in the chamber walls. When the temperature was lowered to -58°C both the transmitter and the microphone were operating satisfactorily. The amplified sinesignal was disconnected from the transmitter and the temperature of the diaphragm allowed to cool down to that of the ambient air (-57°C). When the transmitter signal was reapplied after some 15 minutes, the transmitter resumed normal operation.

With an acoustic pathlength of some four inches, the amplitude of the received microphone signal was found to be sufficient for operation at least down to 10 torr (corresponding to an altitude of about 30 km). Furthermore, the observed phase difference between the transmitted and received signals, as displayed on a dual-beam oscilloscope during the environmental test, did not seem to be a function of pressure. This agrees with Chen's (1981) findings as noted in chapter 4.

The chassis box containing the electronic components was placed in the temperature chamber and found to operate satisfactorily down to -20°C. When the temperature, as measured inside of the box, was lowered to -22°C the instrument malfunctioned. The reason for the malfunctioning seemed to be failure of the microphone power supply due to the alkaline batteries being too cold. However, when the temperature of the instrument increased

to -15°C normal operation resumed.

It is important to recall that due to radiation heating in the atmosphere the temperature of the chassis box is not expected to fall as low as -20°C. Experience from previous launches indicate typical gondola temperatures of around 0°C at altitudes of 20 to 30 km's. Also, as noted in the previous chapter the dissipative heating from the voltage regulators causes the chassis box to be at a temperature considerably above that of the surrounding medium, and thus it is not thought that cooling of the electronic components and power supply presents a serious problem.

For calibration of the flight instrument the chassis-box was positioned outside of the temperature chamber, which thus contained only the transmitter and microphone, as well as the temperature sensors used for reference. This was done to obtain a more uniform temperature field and slower changes of the air temperature in the acoustic path. For a picture of the calibration set-up see figure 14.

The temperature sensors used were; 3 copper-constantan thermocouples (wire diameter of about 1 mm), 1 iron-constantan thermocouple (#40, wire diameter of about 0.05 mm), 2 thin film and 2 bead thermistors*.

Initially all eight temperature sensors agreed (during set-up and adjustment of the acoustic path, with T_o = 25°C). However, once the temperature was lowered it soon became evident that the above temperature sensors had a much slower response to temperature changes than that indicated by the output of the flight instrument with equation (20).

*(Omega Products, Hartford, Connecticut).

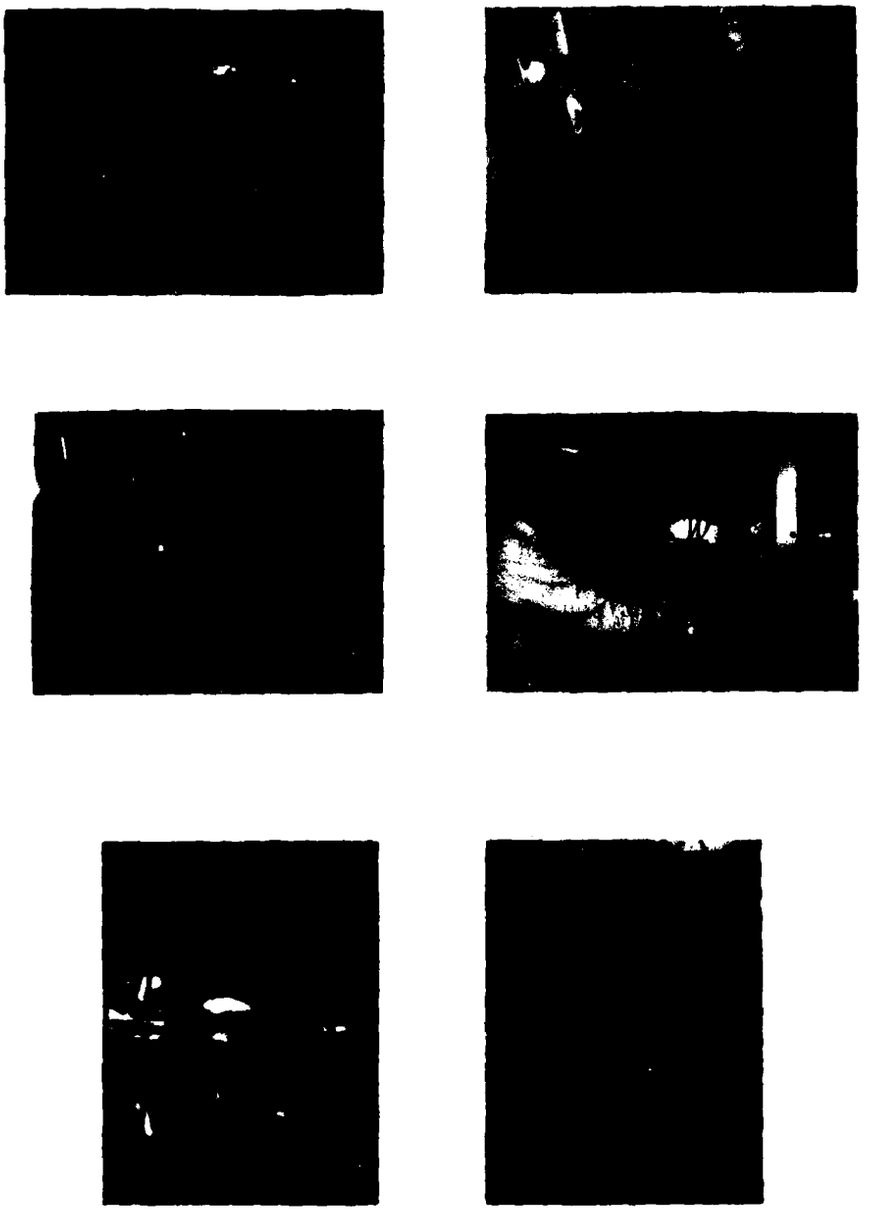

Figure 14. The set-up for calibration at AFGL

The problem of slow response of the thermocouples and thermistors remained at all temperatures. In particular, when cooling the chamber down the discrepancy was found to be large. Consequently, all calibration data was taken while the air in the chamber was allowed to warm up from a minimum temperature by conduction through the chamber walls.

The resulting calibration data, with the linear estimate and the prediction of equation (20), is given in figure 15. It should be noted that the difference between the experimental points, which were obtained using thermocouple readings, and the theoretical estimates is less than the difference between different thermocouples and thermistors (which at times read as much as 10 to 15°C differences.)

It must also be remembered that equation (20) is a one-dimensional result, assuming a point source transmitter. In reality the transmitter is of finite size (4" diameter) and any accurate theoretical prediction would be, at best, complicated.

Therefore, it is believed that the discrepancies do not point to any deficiency of the instrument, but rather show that measurement of the sound speed indicates temperture changes much more rapidly than does the thermocouples and thermistors employed.

In order to resolve this problem satisfactorily additional calibration using finer thermocouples would be necessary. However, since the launch-date for the planned first flight test of the instrument is approaching rapidly it was decided to postpone this until after the flight. Two possibilities exist for obtaining a reference for the data of the first flight.

(1) Attempts to calibrate will be made at the launch site (Holloman AFB, New Mexico). Since the night and day temperatures may fall down

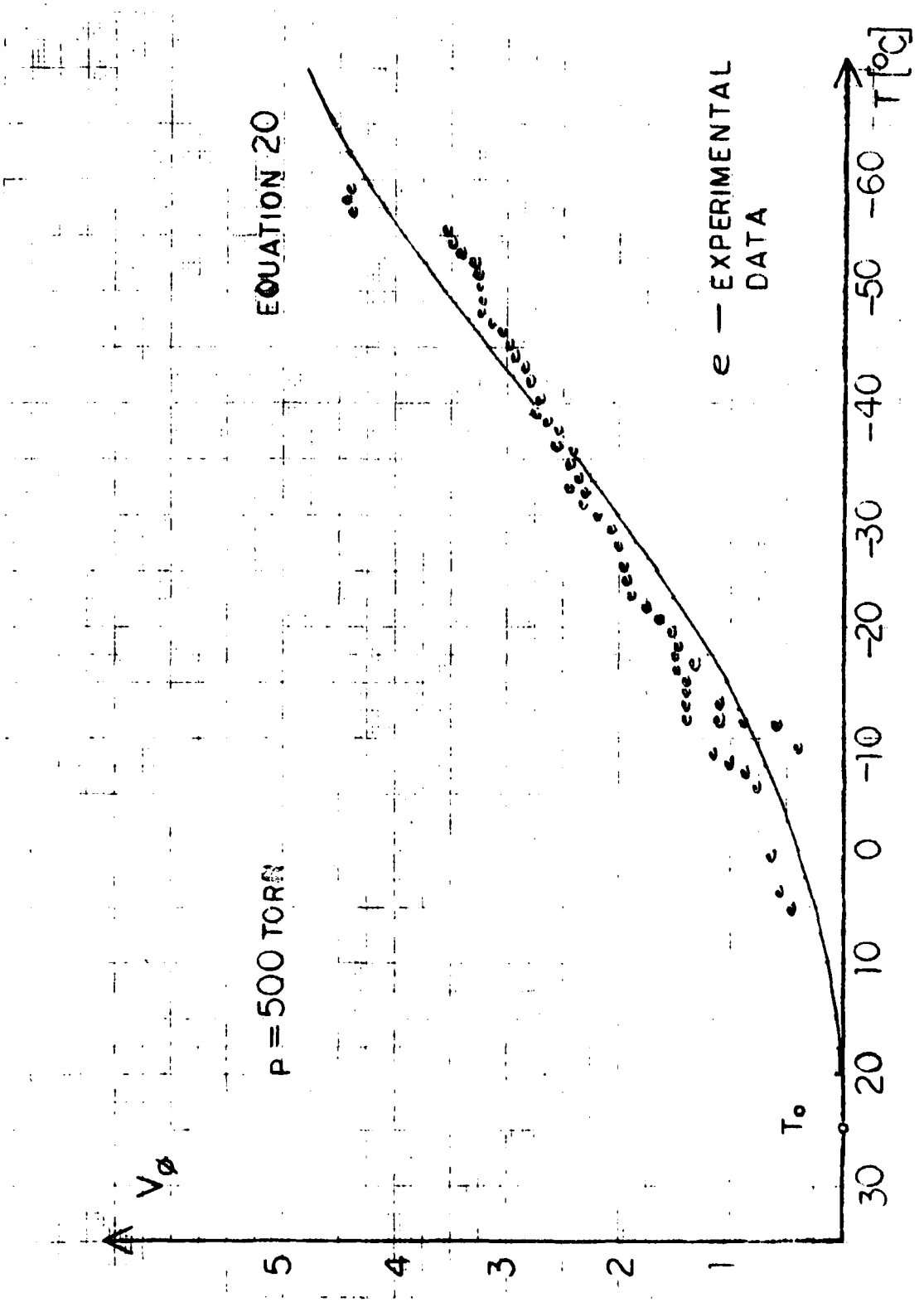

Figure 15. The results of calibration with theoretical predictions

below freezing and reach 25 to 30°C respectively a partial calibration curve could be constructed.

(11) The one dimensional analysis leading to equation (20) could be used as a "best approximation" during the first flight.

It would be necessary to choose some reference temperature, To, and calculate the resulting λ_o; adjust the length of the acoustic path to make the phase difference between the comparator inputs, ϕ_T, zero. Then, measuring the length of the acoustic path, d, we could apply equation (20) to find the air temperature from the dc-level telemetry signal.

This has been done for T_o = 25°C and d = $2\lambda_{25}$ for every degree centigrade from +29° to -84°C. The result of the "theoretical calibration" is plotted in figure 13, detailed results can be found in Appendix IX.

Since the position of the transmitter and microphone in the aforementioned craddle is thought to slightly alter the phase characteristics of the acoustic path, it will be necessary to carry out the final calibration once this craddle is available from AGFL.

Furthermore, it is proposed to calibrate the digital phase signal against the dc-signal during the first flight.

8. METEOROLOGICAL SIGNIFICANCE

At this stage it seems appropriate to quote from one of the earliest papers on sonic thermometry. In 1948, Earl Barret and Verner Suomi of the University of Chicago undertook a study sponsored by the Signal Corps Engineering Laboratories to develop ". . . practical equipment which can be utilized in routine balloon soundings from the ground to altitudes of about 30 km." The instrument they developed used short pulses of high frequency sound,generated by applying a pulse voltage to a piezo-electric crystal. Whether their laboratory model was ever balloon-launched is not known to the present author, but in their 1949 J.A.M. paper they sum it up beautifully:

> Having shown that it is possible to automatically and remotely measure the velocity of sound at various levels throughout the free atmosphere, it becomes desirable to indicate those special advantages which accrue from the use of this technique as contrasted with other methods of temperature measurement now employed. The foremost of these advantages, from the viewpoint of higher-atmosphere sounding, arises from the almost complete indifference to radiation effects resulting from the sonic technique. All existing thermometer devices with which the writers are acquainted make use of some piece of matter as a measuring element, with the assumption that this piece of matter is in thermal equilibrium with the atmosphere in its vicinity. The actual measurement involves a determination of the numerical value of some physical variable quantitiy within this piece of matter, with the supposition that a unique correspondence exists between this variable (electrical resistance, volume, density, thermal e.m.f, etc.) and the "temperature" of the surrounding air. Because of the fact that thermometers of these types have been most useful practically, physicists and engineers have defined "temperature" in terms of these physical variables inside the piece of matter used in the thermometer.
>
> Experience indicates that for a very large number of applications these techniques and definitions are satisfactory. For the case of atmospheric temperature in particular, however, care must be exercised, since the piece of matter may be acted upon by two principal physical variables. The first of these is the air temperature, which for purposes of this paper will be

defined as being directly proportional to the mean translational kinetic energy for a large number of air molecules. In the absence of any other physical forces or energies, experience and thermodynamic considerations indicate that the molecules composing the thermometer will, in time, acquire energy from the air until the net transfer of energy between air and thermometer approaches zero. Under these conditions, the internal properties of the thermometer may be considered as uniquely determined by the energy of the surrounding air, i.e., the air temperature. However, as the instrument ascends higher into the atmosphere, the number of molecules which can exchange energy with the thermometer decreases, while another physical factor, namely radiant energy from the sun, becomes more prominent. This radiation is capable of supplying energy to the thermometer quite independently of the effect of air molecules. In the limiting case, the effect of air molecules approaches zero and the "thermometer" becomes a pyrheliometer or bolometer and measures "temperature" at which energy gained by radiation equals that lost by radiation. Thus it is clear that two conflicting definitions of temperature at a point in the atmosphere can exist and that ordinary thermometers cannot clearly distinguish between them. Practical devices such as radiation shields and highly reflective coatings serve to reduce this ambiguity but cannot entirely eliminate it.

In contrast to the conventional thermometer, the sonic thermometer yields a measurement based upon the very property which is used to define molecular temperature, namely the molecular energy of the air. Since it is unnecessary to utilize an intermediate step involving the internal properties of a piece of matter, the ambiguity in the meaning of "temperature" is reduced. Thus the introduction of sonic thermometers would tend to reduce the confusion which confronts physicists of the upper atmosphere who attempt to abstract information from ordinary radiosonde data at high levels.

The second major advantage may be considered as a corollary of the first. Since no piece of matter acts as an intermediary in the measurement, the time lag associated with ordinary thermometers is not inherent in the sonic technique. No transfer of "heat energy" from air to thermometer, with the usual exponential relationship to time, is required. A time lag does exist, but the magnitude of this lag is of the order of 0.001 sec; that is, the time required for one pulse to travel the fixed distance. Thus, the sonic technique is highly suited to measurements of temperature where the temperature varies widely in short time intervals. This feature makes the technique invaluable for micrometerological studies of temperature variations.

A third advantage obtainable by the sonic technique involves the property of space integration which is inherent in the method. Because of the high velocity of sound waves it is possible to lengthen the distance through which the sound travels to fairly large values, of the order of hundreds of meters. If the atmosphere through which the sound passes is not homogeneous in temperature, the temperature indicated by the sonic method represents an average over the travel distance. The integration cannot be considered as absolutely independent of time, of course, since the velocity of sound cannot be infinite; however, the time interval over which the integration is made is so small in comparison with the rapidity of local temperature fluctuations in the atmosphere that for practical purposes the measurement may be regarded as a space integration made at a particular instant of time. Such space integrations may be of value in determining representative surface temperatures of air masses by elimination of the local effects which affect "spot" temperature measurements at weather stations and by at least a partial averaging of such variations in temperature as are due to local ground heating and/or turbulent motion along the path.

9 CONCLUSIONS AND RECOMMENDATIONS

An airborne sonic thermometer has been designed and developed and now appears ready for testing in the atmosphere. Flight tests, using balloons to carry the instrument to altitudes of 25 to 30 kilometers, are planned.

The instrument incorporates a specially developed electro-magnetic transmitter, a very sensitive condenser microphone, integrated circuit components and a small power amplifier. The balloon launched instrument consists of an aluminum chassis box with a purpose-built craddle holding the transmitter and microphone on the end of a four foot retractable arm.

Tests have shown that the intensity of the sound produced by the transmitter makes the instrument capable of operation to altitudes of at least 30 kilometers. Also, the components of the instrument are thought to be able to withstand the changes of ambient temperature met in flights to these altitudes.

The instrument produces information about the ambient temperature in three different forms

(1) A dc-voltage level varying between zero and five volts.

(2) A digital 250 bit signal.

(3) Two phase shifted 500 Hz signals.

The sensitivity of signal (1), as indicated both by theoretical calculations and by calibration is thought to be about 0.2°C over a temperature range of 105°C, from +25°C to -80°C.

The corresponding sensitivity of the digital signal will be some 0.8°C; whilst the sensitivity of 500 Hz waves will be determined by the chosen method of signal processing.

The temporal resolution of the instrument is set by the transmitter frequency, 8 kHz. However, for balloon launched operations the telemetry of the signals back to ground will be a practical limit. In the first scheduled flight the telemetry rate has been set at two hertz for signal (1) and one hertz for signal (2), whilst signal (3) will be transmitted continuously.

In its present form the instrument suffers from the effect of velocity contamination of the measured acoustic propagation velocity which can cause errors of up to one degree centigrade in the measured temperature. To eliminate this error it is proposed that a second sound path, with an acoustic signal of a suitably spaced frequency to avoid signal crosstalk, be incorporated in the next design. This would allow simultaneous measurements of the ambient velocity and temperature and accurate determination of quantities like flux Richardson number and turbulence structure-constant should be possible.

Another difficulty concerns the need for a better calibration technique. The available calibration, whilst confirming the overall response and measuring range, is too erratic and unrepeatable to be used for accurate temperature determination. Thus it is proposed that during the first flight the instrument be calibrated outdoors on site, or, failing this, that the theoretical response for a point source transmitter be used in lieu of a good calibration curve. Future work should be focused on developing a good method of calibration; possibly by using very fine thermocouple wire probes and a very large chamber.

In summary it may be concluded that the present instrument should be capable of delivering measurements of the ambient air temperature with an

accuracy of ± 0.1°C at a rate determined by the telemetry frequency, up to 8000 times per second. It should constitute a major improvement over other procedures for obtaining airborne atmospheric temperature measurements due to its indifference to radiative heating, its ability to spatially integrate over the acoustic path to obtain more representative values of the air temperature and its extremely rapid time response.

Acknowledgements

I would like to take this opportunity to thank everybody that, in some way or other, helped me complete this thesis. Mentioning every name would be impossible but some of the important ones in the Aerophysics Lab were...

...my advisor, Dr. Charles W. Haldeman, who guided me though my first stumbling steps in electronic design and always remained a source of information and inspiration.

...Professor K. Uno Ingard who helped initiate the project and was the ultimate reference on any problem concerning acoustics.

...Gautham Ramohalli, who in a very real sense endured the frustrations associated with electronic design -- through sharing the same office -- and who devoted much time in chasing "electronic bugs." Gautham also designed the digital phasemeter described in chapter 6.

...James Nash for all his help, and for always knowing where to locate that particular little "gizzmo."

...Victor Dubrowski for all the excellent machine work he did, and for always finding time to do it in impossibly busy hours.

In transforming the prototype into a flight instrument I got great help from a lot of people at the Airforce Geophysics Lab. In particular from...

...Edmund Murphy of the Atmospheric Composition Branch, who not only funded the project, but who also worked very hard to complete it, and kept things going by his belief that we could make it.

...Hans Lapping, Ron Lavigne and Ken Murphy of the Balloon Instrumentation Branch who came up with the all-important diaphragms for the transmitter, and also made available their facilities for printed circuit-board production, their vast stock of electronic components and lots of advice.

...Richard "Dick" Borgesen of the Mechanical design group who designed the support arm and craddle for the acoustic components, and did an excellent job of it.

Other people who deserve particular mention include...

...Maureen Ahern of M.I.T.'s Purchasing office, who was most helpful in locating those 'hard-to-find" electronic components.

...Jim Lange of Exar Integrated Systems, Sunnyvale, California, for his advice on uses of Exar components.

...Gary Langdon of Northern Engineering Laboratories, Burlington, Wisconsin, who made the initial design for the crystal controlled signal generator.

...Doreen Antonelli and Paul McLaughlin of the MIT Word Processing Center for skillful use of their "machine".

Many names, lots of help. To all of you, thank you!
Mentioning these names I do of course not try to involve them in any error associated with this thesis, for which I bear full responsibility.

In closing, since this is the last thesis to come out of the now defunct Aerophysics Laboratory, I would like to close in honor of "the lab." It's sad to see it go.

References

Barret, E.W. and Suomi, V.E. (1947).
Preliminary report on temperature measurement by sonic means.
J. Meteor., 6, pp. 273-276.

Chen, Z.Y. (1981).
Feasibility study of acoustic thermometry in the upper atmosphere.
Master's Thesis, M.I.T., March 1981.

ICAO (1962).
U.S. Standard Atmosphere, 1962.
NASA, USAF, USWB.

Kaimal, J.C. and Businger, J.A. (1962).
A continuous wave sonic anemometer - thermometer.
J. Appl. Meteor., 2, pp. 156-164.

Kneser, H.O. (1933).
Schallabsorption in mehratomigen gasen.
Ann. Physik, 16, pp. 337-348.

Lancaster, D. (1975).
Active filter cookbook.
Howard W. Sams and Co., Inc., Indianapolis, Indiana.

Larsen, S.E., Weller, F.W. and Businger, J.A. (1978).
A phase-locked loop continuous wave sonic anemometer-thermometer.
J. Appl. Meteor., 18, pp. 362-368.

Lichfield, E.W., and Carlson, N.E. (1967).
Temperature control of balloon packages.
NCAR, TN-32, Boulder, Colorado

Morse, P. and Ingard, K.U. (1968).
Theoretical acoustics
McGraw Hill, New York

Information pertaining to the development of the present instrument has appeared in the following reports published at M.I.T.'s Aerophysics Laboratory --

ALP 79-16 Work statement (Dec. 79)
Quarterly progress report #1 (Sep. 80)
#2 (Dec. 80)
#3 (Mar. 81)
#4 (Jun. 81)
#5 (Sep. 81)
#6 (Dec. 81)

AR 1042 (Feb. 81)
1044 (May 81)
1045 (Aug. 81)

Specifications on the acoustic and electronic components can be found in product information from the following companies --

Bruel & Kjaer, Naerum, Denmark
Exar Inc., Sunnyvale, California
Lamotite Products, Cleveland, Ohio
Motorola Semiconductor Products, Pheonix, Arizona
Rotron, Torque systems, Watertown, Massachusetts

Other references on sonic anemometry and thermometry include --

Beaubien, D.J., Bisberg, A. and Pappas, A. (1967).
Design, development and testing of an acoustic anemometer.
Final rept., AFCRL-66-650, Cambridge Systems Inc., 48 pp.

Bovsheverov, V.M., and Voronov, V.P. (1960).
Acoustic anemometer.
Izvestia Geophys. series, 6, 882-885.

Corby, R.E. (1950).
Acoustic anemometer - anemoscope.
Electronics, 23, (1), 88-90

Fox, H.L. (1968).
Continuous wave three-component sonic anemometer.
Final rept., AFCRL 68-0180, Bolt, Beranek and Newman, Inc., 57 pp.

Friehe, C.A. (1976).
Effect of sound speed fluctuations on sonic anemometer measurements.
J. Appl. Meteor., 15, 607-610.

Kaimal, J.C. (1966).
The analysis of sonic anemometer measurements from the Cedar Hill tower.
Environ. Res. Paper, AFCRL 66-542, 153 pp.

Kaimal, J.C., Haugen, D.A. and Newman, J.T. (1966).
A computer-controlled mobile micrometeorological observation system.
J. Appl. Meteor., 5, 411-420.

Kaimal, J.C., Wyngard, J.C. and Haugen, D.A. (1968).
Deriving power spectra from a three-component sonic anemometer.
J. Appl. Meteor., 7, 827-837.

Mitsuta, Y. (1966).
Sonic anemometer-thermometer for general use.
J. Meteor. Soc. Japan., 44, 168-172.

Mitsuta, Y., Miyatse, M. and Kobori, Y. (1967).
Three-dimensional sonic anemometer-thermometer for atmospheric turbulence measurements.
Disast. Prev. Res. Inst., Kyoto Univ., WDD Tech note, Japan.

Mitsuta, Y. (1971).
Development of the sonic-anemometer thermometer and its applications.
Final report, WDD Tech. note no. 6, Disastr. Prev. Res. Inst., Kyoto Univ., Japan.

Schotland, R.M. (1956).
Measurement of wind velocity by sonic means.
J. Meteor., 12, 386-390.

Suomi, V.E. and Businger, J.A. (1959).
Principle of the sonic anemometer-thermometer.
AFCRC-TR-58-235, Geophys. res. papers, no. 59, 673 pp.

APPENDIX I

THE EFFECT OF HUMIDITY ON THE MEASURED TEMPERATURE

From the Smithsonian Physical Tables, the vapor pressure of air (P_A) and water (P_W) was obtained for different relative humidities.

Then, the gas constant for humid air -

$$R_{\%} = (M_A/M_{\%})\, R_{Dry\ air}$$

- where -

$$M_{\%} = (P_A M_A + P_W M_w)/P_{Total}$$

M_A = Molecular weight of dry air

M_W = Molecular weight of water

P_{Total} = 760 mm Hg (Approximate: P_{Total} = constant)

We have the percentage change in the sound speed -

$$c_{\%}/c_{Dry} = (R_{\%}/R_{Dry})^{1/2}$$

- from which the change in the telemetry signal, and hence the error in the temperature information, can be calculated.

This gives -

$T_{Ambient}$	Humidity	$c_{\%}/c_{dry}$	ΔV_{ϕ}	ΔT_{error}
30°C	100% relative	1,0080	98mV	2°C
20°C	"	1,0045	72mV	1.4°C
0°C	"	1,0011	13mV	0.25°C
-50°C	"	1,0000	0	0

(using $\Delta T/\Delta V_{\phi} = 0.2$ °C/10mV)

From the US Standard Atmosphere tables we have -

$$T_{5km} = -17.5°C$$
$$T_{11km} = -56°C$$

Thus, this effect is seen to be unimportant in the upper atmosphere. It should, however, be kept in mind at low altitudes and on the ground.

Appendix II

THE EFFECT OF VELOCITY FLUCTUATIONS ON THE MEASURED TEMPERATURE

The present design is intended for use as a balloon launched instrument, and we must therefore take into consideration the velocities in the soundpath that are associated with such operation.

The windspeed perpendicular to the soundpath, W, will arise from two sources. During ascent or descent of the balloon it will consist mostly of the rate of change of altitude. When the balloon is making measurement at the pre-determined ' float-altitudes' it will be due to gusts in the mean wind direction. Assuming an ascent rate of 6 m/s and a sound speed of 295 m/s - the lowest sound speed in a flight to 25 km altitude, which will give the largest relative error for a given wind speed - we find that the contaminated temperature reading is some 0.1°C below the true temperature.

If we take 10% as a maximum turbulence level encountered by the balloon and assume that the mean wind is not greater than 50 m/s (112 mph!) we find that the effect of W while the balloon is floating is even less, and hence we neglect it.

Splitting the wind velocity along the soundpath up into its mean and fluctuating components - $U = \overline{U} + U'$ - we note that $\overline{U}$ will have no effect on the measured temperature since the balloon is assumed to move with the mean wind. However, U', the fluctuating part of the wind along the soundpath, is of concern, as it will add linearly to c in equation (11) in the text.

The gondola is spherical of roughly 12 feet diameter, and made of aluminum tubing, with the transmitter and receiver positioned some 4 feet away from it. Typical Reynolds numbers based on the gondola diameter will be between one hundred thousand and one million depending on the gusts, and the soundpath will be in a mainly turbulent flowfield.

Also, the frame of the gondola will scatter the gusts and produce additional turbulence.

The error in the temperature reading has been calculated, assuming again 10% turbulent intensity. Some typical values are displayed -

T	U'~ 0.1U	c	$T_{Apparent}$	ΔT_{Error}
	Away from gondola			
-56.4°C(T_{min})	$1^m/s$	295 m/s	-55.1°C	1.3°C
"	$3^m/s$	"	-52.0°C	4.4°C
"	$5^m/s$	"	-49.1°C	7.3°C
	Towards gondola			
"	$-1^m/s$	"	-57.9°C	-1.5°C
"	$-3^m/s$	"	-60.8°C	-4.4°C
"	$-5^m/s$	"	-63.7°C	-7.3°C

The Reynolds number quoted is based on the gondola diameter (d = 12 feet) -

$$Re_d = \frac{u'd}{\nu} \sim 1 \cdot 10^6 - 1 \cdot 10^7$$

Appendix III

THE TEMPERATURE RANGE FOR VARIOUS CHOICES OF REFERENCE TEMPERATURE AND PATH LENGTH

We will consider four different alternatives for pathlength and reference temperature

(1)

Reference temperature T_o = 25°C = 298K

Propagation velocity and wavelength at reference temperature

$$c_o = [\gamma R T_o]^{1/2} = 346.4\ ^{m}/s$$

$$\lambda_o = {}^{co}/f = 4.33\ cm$$

where the signal frequency is constant f = 8000,0 H_z

Pathlength $d = 2\lambda_o = 8.66$ cm

Thus, at $T=T_o$ the phase difference across the acoustic path is zero.

The minimum temperature that can be measured unambiguously will cause a phase difference of 180 degrees. That is, when -

$$d = (2 + 1/2)\lambda$$

or

$$\lambda_{min} = \frac{2}{5} d = 3.46 \text{ cm}$$

Thus, the minimum propagation velocity and temperature

$$c_{min} = \lambda_{min} \cdot f = 277 \text{ m/s}$$

$$T_{min} = 190.7K \simeq \underline{-82°C}$$

ie - for this pathlength the dc-voltage output from the phase comparator will decrease from it's maximum to its' minimum value as the air temperature changes from plus 25 to minus 82 degrees centigrade. If the temperature falls further the dc-voltage will increase again and cause ambiguity.

However, the digital phasemeter can measure over a full cycle (360°) and would therefore give unambiguous readings down to $\underline{-141°C}$.

In exactly the same manner we find

(2) Reference conditions $T_o = 20°C \simeq 293K$

$c_o = 343.5$ m/s

$\lambda_o = 4.29$ cm

Pathlength $d = 3\lambda_o = 12.88$ cm

Minimum when $d = (3 + 1/2)\lambda$

$\lambda_{min} = 2/7\ d = 3.68$ cm

Ie $c_{min} = 294.4$ m/s

$T_{min} = 216K = \underline{-58°C}$

(3)

Reference $T_o = 0°C = 273K$

Pathlength $d = 4\lambda_o = 16.58$ cm

Minimum $\lambda_{min} = 2/9\ d = 3.68$ cm

$T_{min} = 215K = \underline{-57°C}$

(4)

Reference $T_o = 40°C = 313K$

Pathlength $d = \lambda_o = 4.43$ cm

Minimum $\lambda_{min} = 2/3\ d = 2.95$ cm

$T_{min} = 138,8K = \underline{-134.2°C}$

Or, for the digital phasemeter $T_{min} = \underline{-195°C}$

APPENDIX IV

RELEVANT ATMOSPHERIC PROPERTIES

From tables of the US Standard Atmosphere, and from Chen (1981) for C_{8KHZ}/C_o, we obtain

H (geometric) [KM]	T [°C]	p [mb]	ρ [kg/m^3]	c_o [m/s]	c_{8KHZ}/c_o [-]
Sealevel	15	1013,25	1,225	340.3	1,000
0.5	11.75	954,61	1,167	338.4	"
1	8.50	898,76	1,112	336.4	"
2	2.00	795,01	1,007	332.5	"
3	-4.50	701,08	0,909	328.6	"
5	-17.50	540,20	0,736	320.5	"
10	-50.00	264,36	0,413	299.5	"
15	-56.50	120,44	0,194	295.1	"
20	-56.50	54,75	0,088	295.1	"
25	-51.50	25,11	0,039	298.4	"
30	-46.50	11,72	0,018	301.8	"
35	-36.10	5,59	$8,46 \cdot 10^{-3}$	308.6	"
40	-22.10	2,77	$3,85 \cdot 10^{-3}$	317.6	"
45	-8.10	1,07	$1,93 \cdot 10^{-3}$	326.4	"
50	-2.50	0,76	$9,77 \cdot 10^{-4}$	329.8	"
55	-8.50	0,30	$5,29 \cdot 10^{-4}$	326.1	"
60	-18.50	0,20	$2,85 \cdot 10^{-4}$	319.9	1,001

APPENDIX V

A DESCRIPTION OF A FEEDBACK SYSTEM USING A PHASE LOCKED LOOP INTEGRATED CIRCUIT

Description of the Circuit

The closed loop circuit uses an XR-2212 phase locked loop integrated circuit whose VCO generates a squarewave signal of a frequency determined by the phase and frequency of the input signals to the phase comparator. This squarewave signal, after having been converted into a sine-wave is amplified and used as the input signal to the transmitter.

After having been picked up by the microphone it is fed back through the frequency analyzer as the input to the phase comparator. The reference signal at the phase comparator is the squarewave generated by the VCO and thus the phase difference measured by the phase comparator is determined by the phase lag of the acoustic path (and across the various components through which the signal passes).

The phase comparator produces an error voltage proportional to the phase difference between its inputs

$$V_{\Phi} = K_d \cos \Delta\Phi$$

- where K_d is the phase detector conversion gain and $\Delta\Phi$ the measured phase difference.

This error voltage, after filtering, is the input to the VCO and hence the frequency of the transmitted signal will depend on the phase difference of the acoustic path. Thus changing the acoustic path will cause a change in the transmitted signal in a direction that reduces the phase difference between the transmitter and the microphone.

A simplified block diagram for the closed loop circuit, displaying its operating principle, is given below.

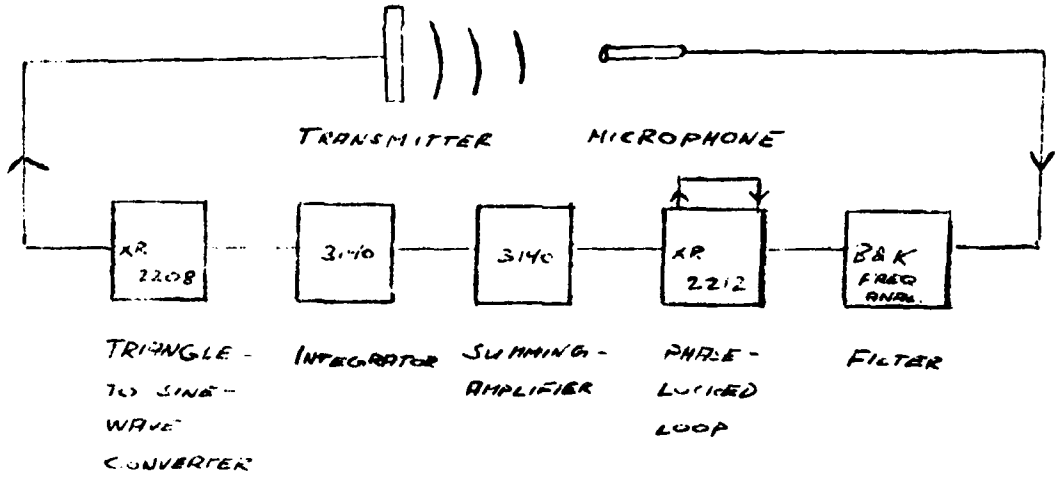

The Performance of the Closed Loop

The lockrange of the phase-locked loop extends from about five to eleven-and-a-half kilohertz.

Considering only the static response of the loop, we find that a temperature fluctuation of 1 K will result in a frequency change of between 4.5Hz and 15 Hz at different altitudes and for frequencies at the two ends of the lock range.

Thus the closed loop does not appear to be as sensitive as the open loop but the frequency change for a temperature change of 1 K is still believed to be sufficient to obtain a temperature resolution of one degree centigrade.

However, this analysis models the locked loop as a linear system and is at best simplified. It does, for instance, not consider its stability.

For more information including circuit diagram and calculation of the circuit parameters see AR 1044 of the Aerophysics Lab, MIT; from which we quote the following conclusion ---

--- the open loop, being a linear circuit as opposed to the non-linear closed loop, is very much simpler to analyze and would thus appear more suitable for the initial design efforts. It would also put less stringent requirements on the acoustic properties of the transmitter and experience none of the problems associated with loop stability.

APPENDIX VI

CIRCUIT DIAGRAMS AND SPECIFICATIONS FOR THE ELECTRONIC COMPONENTS

This appendix contains circuit diagrams and component listings for the following electronic components (in the order listed).

Generator board

Filter board

Comparator board

Digital board

Regulator board

SIGNAL GENERATOR

XR 8038M - SIGNAL GENERATOR (8000 Hz SINE-SIGNAL)

XR 4741M - BUFFER

Y1	NE13-TXY 8000 HZ CRYSTAL	
C1	36 pF DUR-MICA CAPACITOR	
C2	12000 pF CERAMIC CAPACITOR	
C3	"	
R1	549 KΩ	RN60C PRECISION RESISTOR
R2	1 KΩ	"
R3	412 KΩ	"
R4	14 KΩ	"
R5	6.19 KΩ	"
R6	1.91 KΩ	"
R7	12.1 KΩ	"
R8	11 KΩ	"
R9	169 KΩ	"
R10	4.64 KΩ	"
R11	3.74 KΩ	"

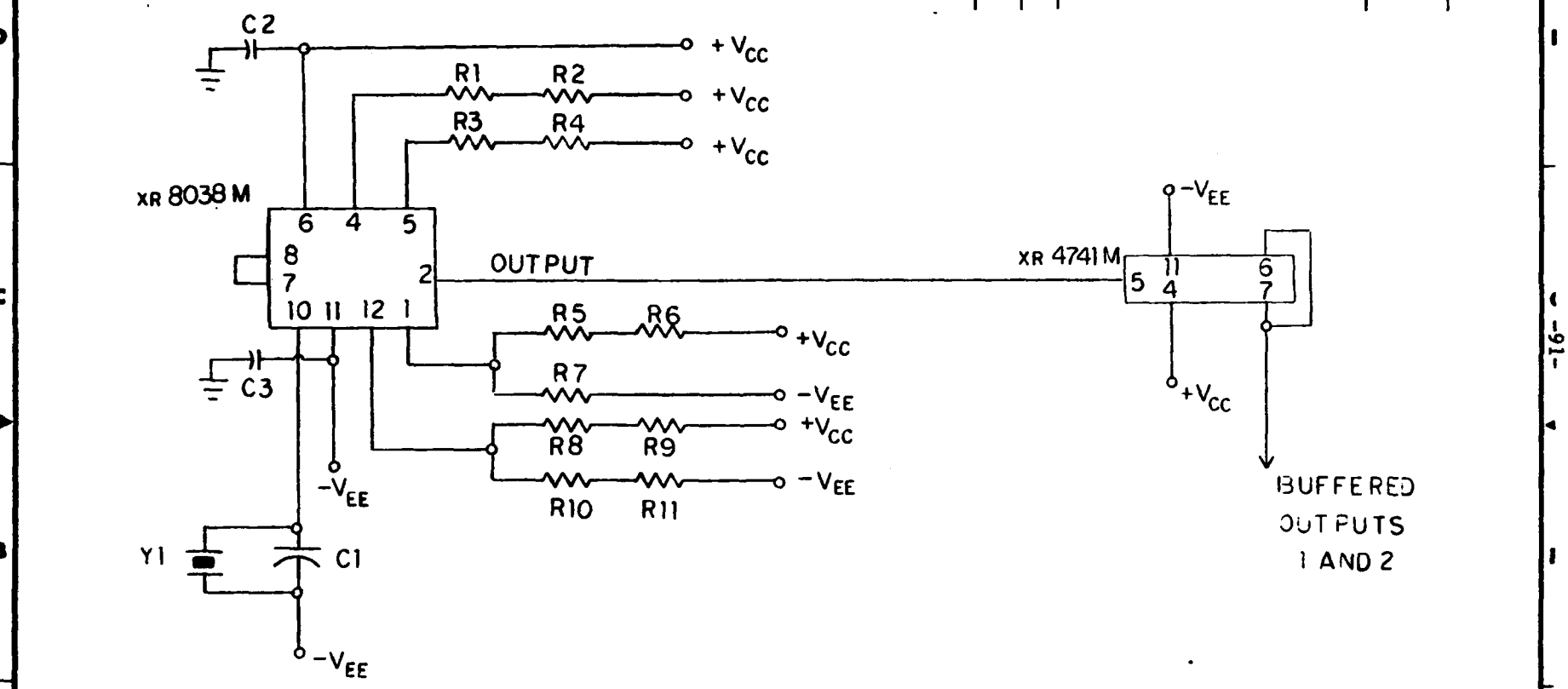

ZONE	LTR	DESCRIPTION	DATE	APPROVED
REVISIONS				

UNLESS OTHERWISE SPECIFIED DIMENSIONS ARE IN INCHES
TOLERANCES ARE
FRACTIONS DECIMALS ANGLES
± .XX ± ±
.XXX ±

MATERIAL

FINISH

NEXT ASSY | USED ON

APPLICATION

DO NOT SCALE DRAWING

CONTRACT NO.

APPROVALS	DATE
DRAWN T.C.	5/5/82
CHECKED	

B.A.T.

SIGNAL - GENERATOR

SIZE	CODE IDENT NO.	DRAWING NO.
B		

SCALE | SHEET OF

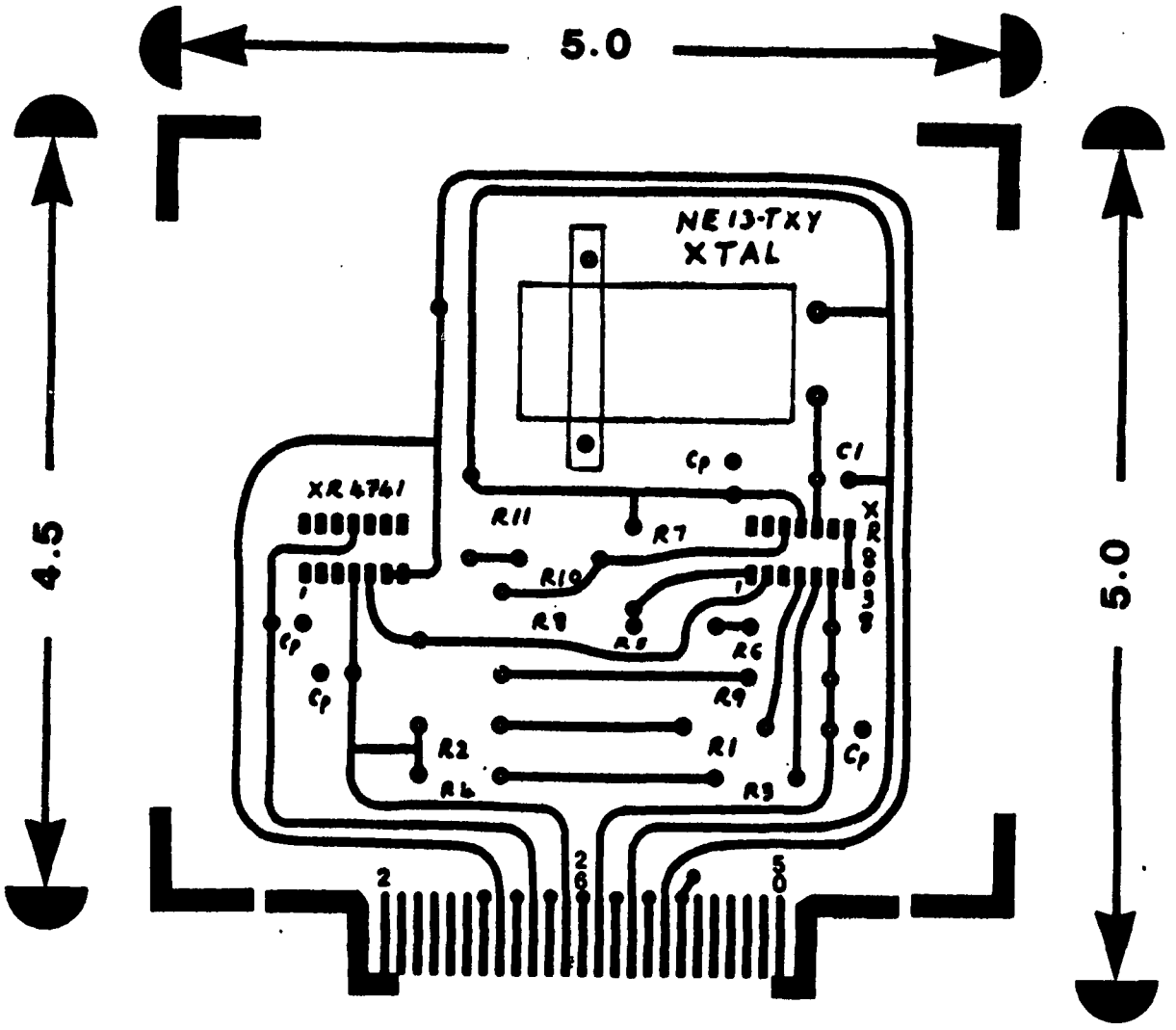

RIGHT READING COMP SIDE

Signal generator board component side

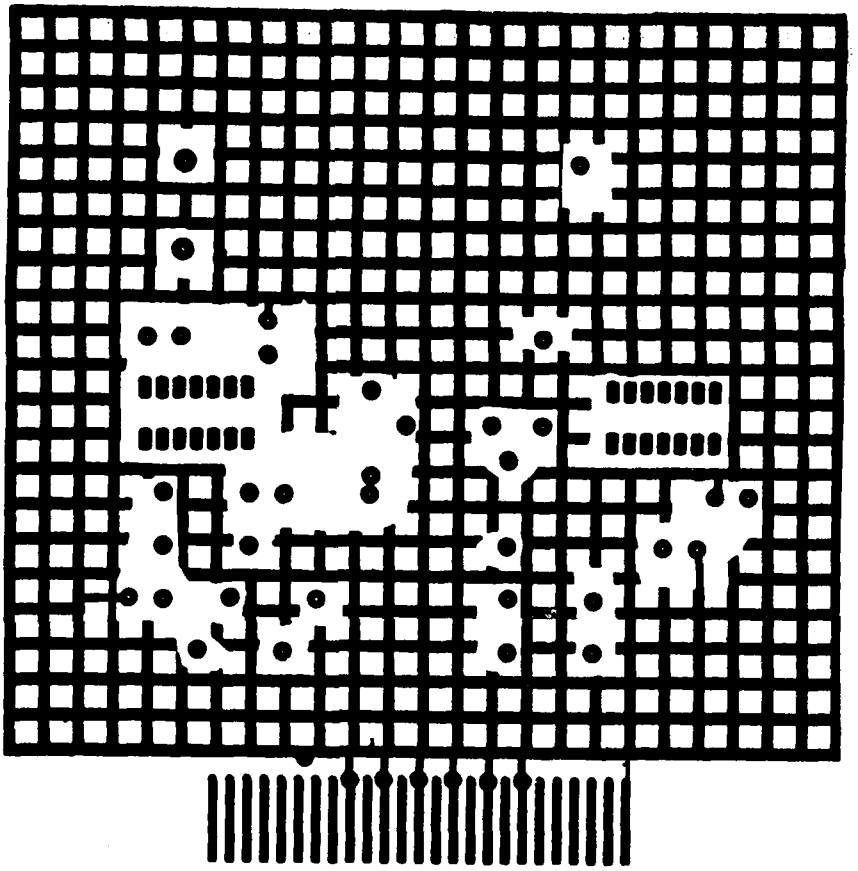

GROUND SIDE

Signal generator board ground side

FILTER

XR 4741	BUFFER	
LM 101	FILTER OP AMP	
C1	2000 pF	DUR-MICA CAPACITOR
C2	5 pF	"
C3	[Removed]	
C4	1 μF	CERAMIC CAPACITOR
R1	3.91 KΩ	RN60C PRECISION RESISTOR
R2	6.01 KΩ	"
R3	9.96 KΩ	"
R4	1.5 MΩ	"
R5	1.5 MΩ	"
R6	9.97 KΩ	"
R7	4.49 KΩ	"
R8	1.5 MΩ	"
R9	9.98 KΩ	"
R10	100.4 Ω	"
R11	301 KΩ	"
R12	1 KΩ	"
R13	9.09 KΩ	"
R14	82.5 KΩ	"
R15	200 KΩ	"
R16	1.5 MΩ	"

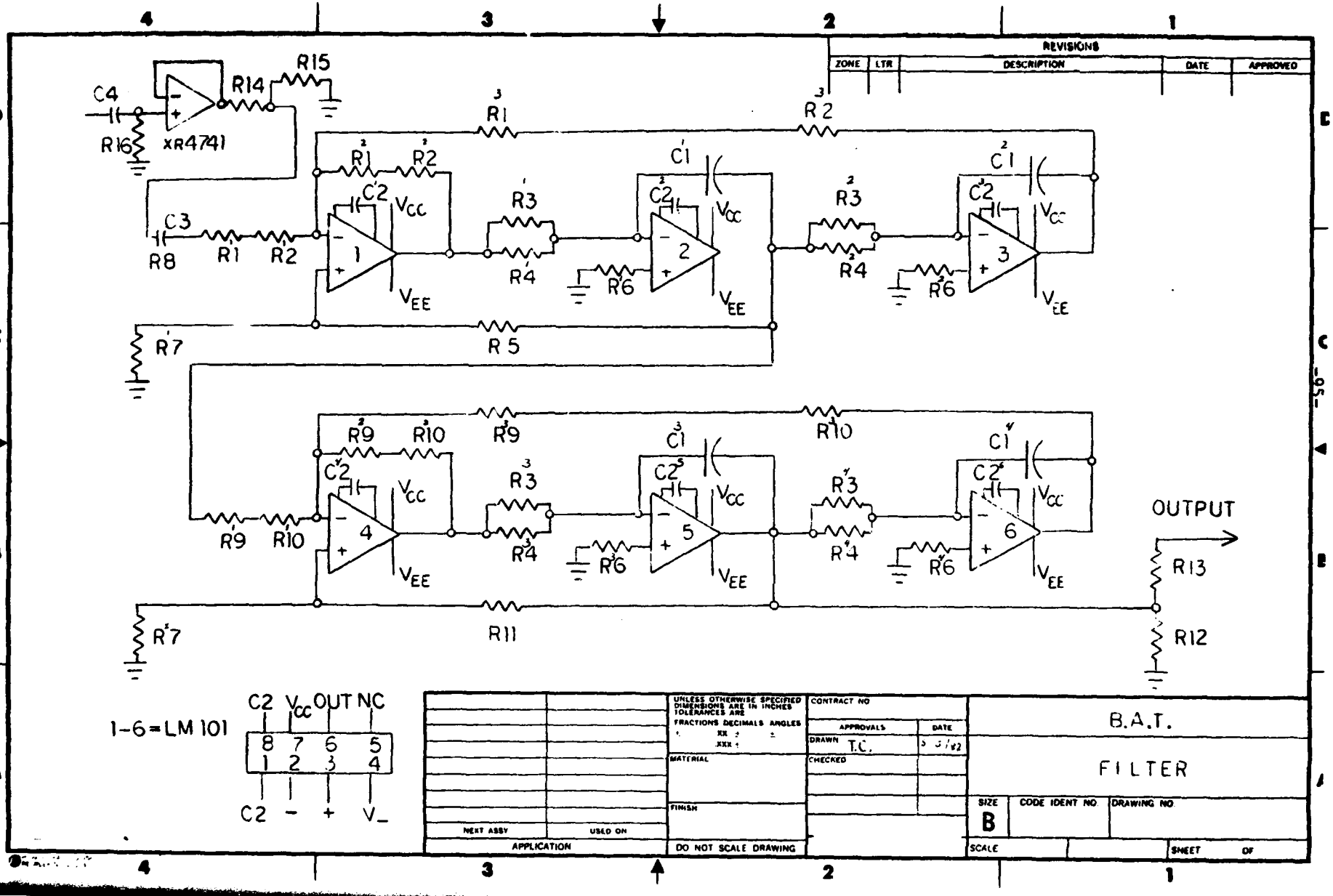
REVISIONS
ZONE
LTR
DESCRIPTION
DATE
APPROVED
C4
R16
XR4741
R14
R15
C3
R8
R1
R2
C2
Vcc
VEE
R3
R4
R6
C1
R5
R7
R9
R10
R11
OUTPUT
R13
R12
1-6=LM 101
C2 Vcc OUT NC
8 7 6 5
1 2 3 4
C2 - + V_
UNLESS OTHERWISE SPECIFIED DIMENSIONS ARE IN INCHES TOLERANCES ARE
FRACTIONS DECIMALS ANGLES
XX ±
XXX ±
MATERIAL
FINISH
NEXT ASSY
USED ON
APPLICATION
DO NOT SCALE DRAWING
CONTRACT NO
APPROVALS
DATE
DRAWN T.C.
3 3/82
CHECKED
B.A.T.
FILTER
SIZE B
CODE IDENT NO.
DRAWING NO
SCALE
SHEET OF

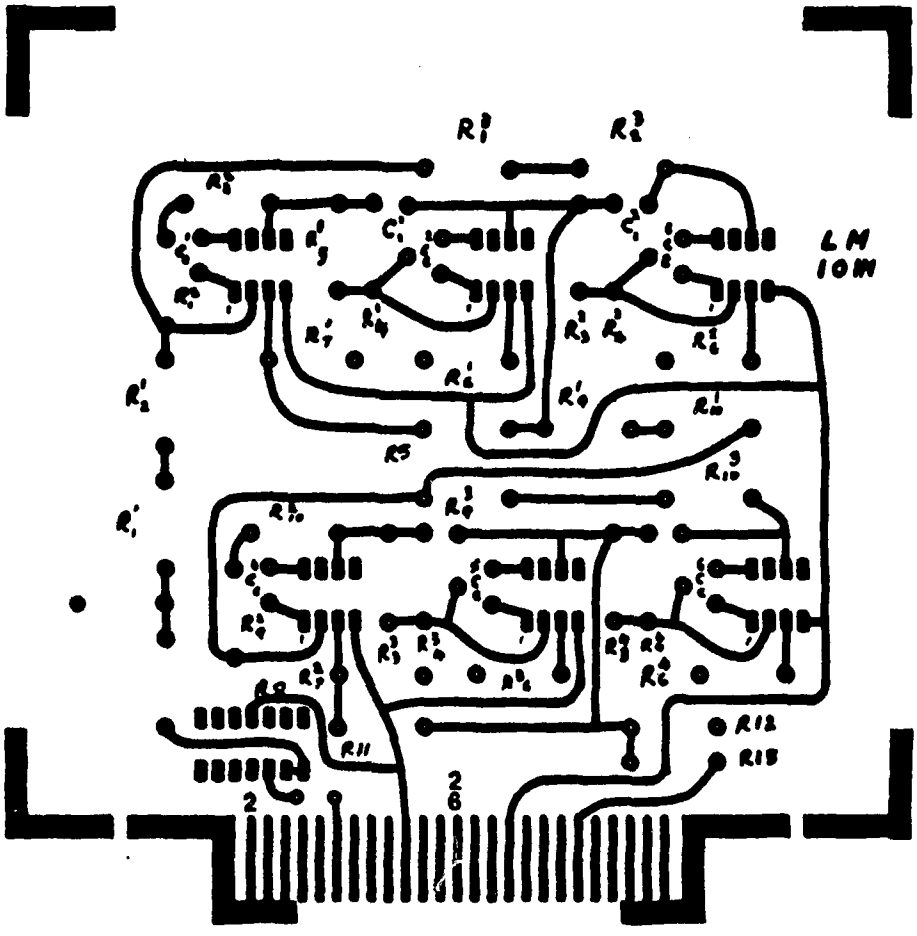

Eight khz bandpass filter board component side

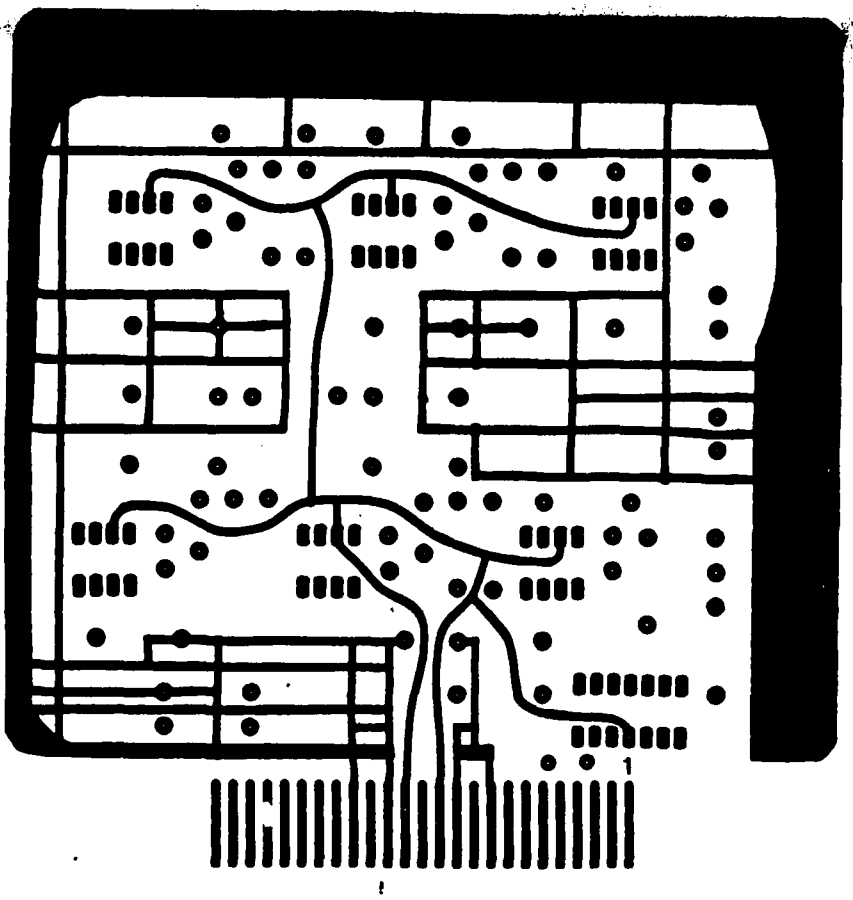

GROUND SIDE

Eight khz bandpass filter board ground side

COMPARATOR

LM 311/111	MOTOROLA VOLTAGE COMPARATOR	MILSPEC
XR 2208 M	EXAR PHASE COMPARATOR	"
MC 14040 B	MOTOROLA 12 BIT COUNTER	"
XR 4741 M	EXAR OP AMP	"

R1	4.99 KΩ	RN 60C	R17	10 KΩ	RN 60C
R2	4.99 KΩ	"	R18	10 KΩ	"
R3	1 KΩ	"	R19	2 KΩ	"
R4	[REMOVED]		R20	2 KΩ	"
R5	3.01 KΩ	"	R21	2 KΩ	"
R6	2 KΩ	"	R22	100 KΩ	RN 65 D
R7	1.5 MΩ	"			
R8	1.5 MΩ	"	C1	330 pF	DUR-MICA CAP.
R9	1.5 MΩ	"	C2	22000 pF	CERAMIC CAP.
R10	1.5 MΩ	"	C3	22000 pF	"
R11	1.5 MΩ	"	C4	10 pF	"
R12	1 KΩ	"	C5	2200 pF	"
R13	2 KΩ	"	C6	1 μF	"
R14	1 KΩ	"	C7	12000 μF	"
R15	3.92 KΩ	"	C8	1 μF	"
R16	10 KΩ	"			

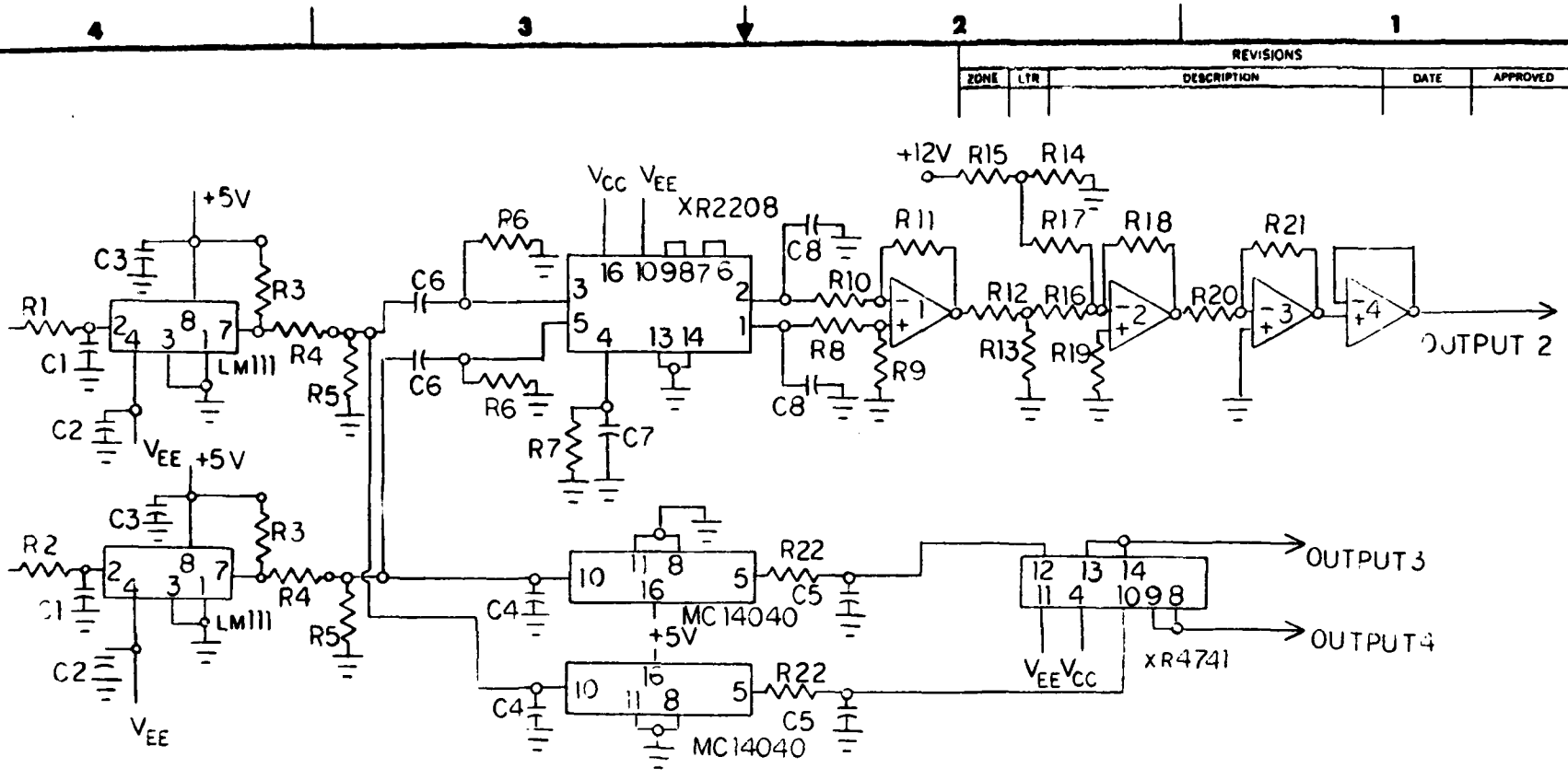

1-4 IN ONE XR4741

REVISIONS				
ZONE	LTR	DESCRIPTION	DATE	APPROVED

UNLESS OTHERWISE SPECIFIED DIMENSIONS ARE IN INCHES TOLERANCES ARE FRACTIONS DECIMALS ANGLES
± XX ± ±
XXX ±

MATERIAL

FINISH

NEXT ASSY | USED ON

APPLICATION

DO NOT SCALE DRAWING

CONTRACT NO

APPROVALS	DATE
DRAWN	
CHECKED T.C.	5/5/82

B.A.T.

COMPARATOR

SIZE B | CODE IDENT NO | DRAWING NO

SCALE | SHEET OF

AD-A118 774 MASSACHUSETTS INST OF TECH CAMBRIDGE AEROPHYSICS LAB F/G 20/1
DEVELOPMENT OF AN AIRBORNE SONIC THERMOMETER.(U)
SEP 82 T R CHRISTIANSEN F19628-80-K-0089
UNCLASSIFIED AFGL-TR-82-0179 NL

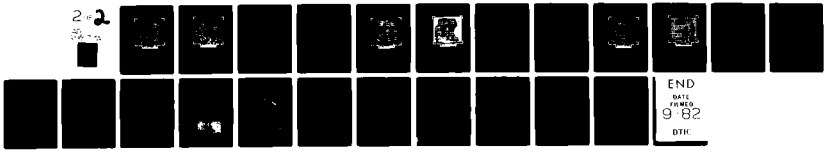

END
DATE FILMED
9-82
DTIC

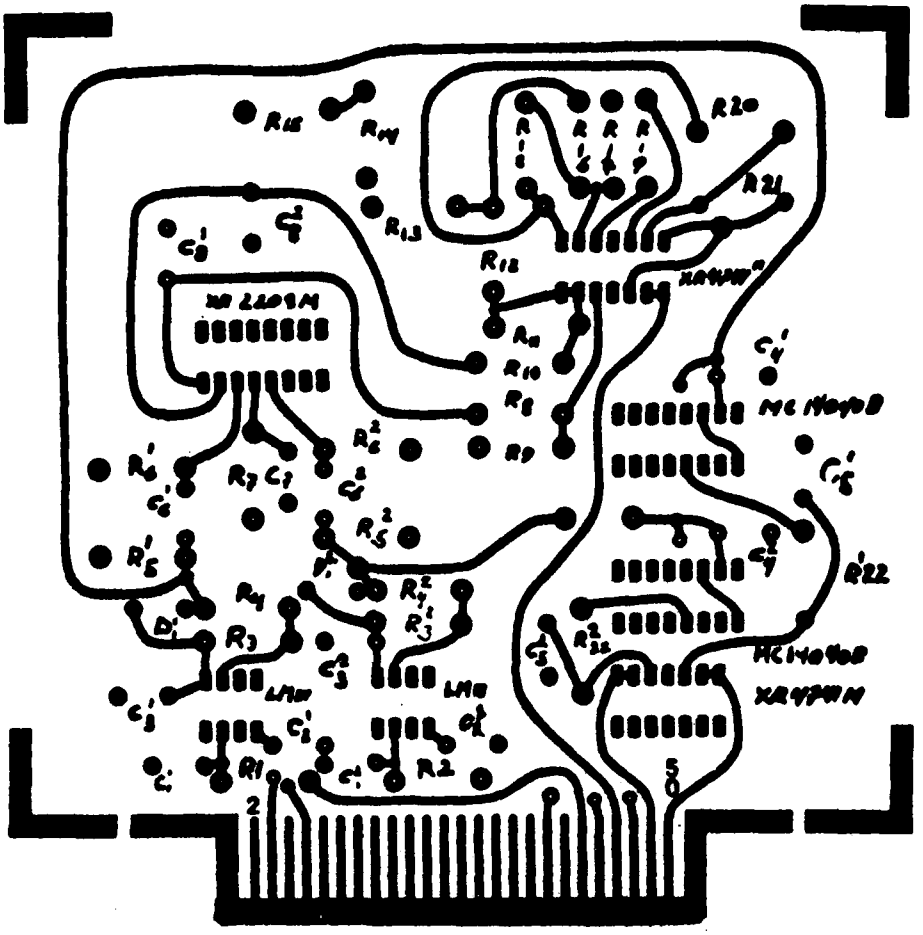

COMPARATOR COMPONENT SIDE

Comparator board component side

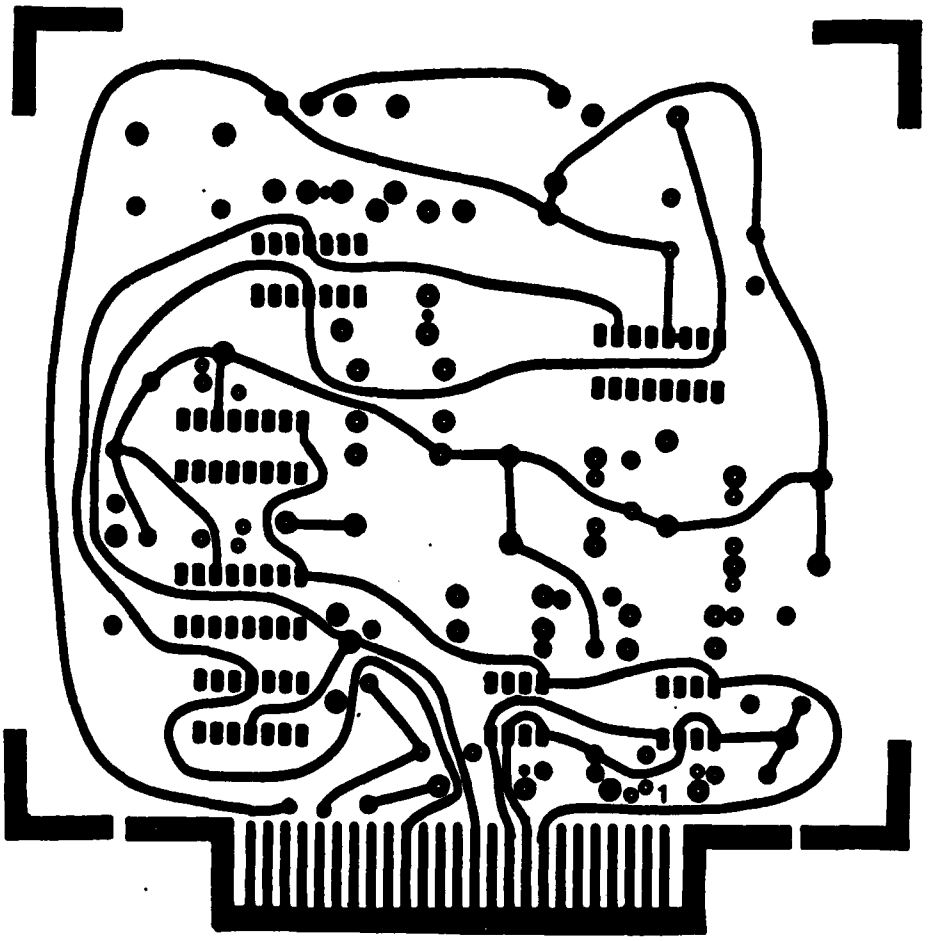

Comparator board ground side

DIGITAL PHASEMETER

MC 14011 B	MOTOROLA	QUAD 2-INPUT NAND-GATE
MC 14013 B	"	DUAL TYPE D FLIP-FLOP
MC 14040 B	"	12 BIT BINARY COUNTER
MC 14042 B	"	QUAD LATCH
MC 14049 B	"	HEX BUFFER
MC 14521 B	"	24 STAGE FREQUENCY DIVIDER
MC 14521 B	"	DUAL COMPLEMENTARY PAIR PLUS INVERTER

8 MHz CRYSTAL

R1	3.3 KΩ	CARBON RESISTOR 5%
C1	330 pF	DUR-MICA CAPACITOR
C2	330 pF	"

(Miscellaneous capacitors from V_{CC} and V_{EE} to ground)

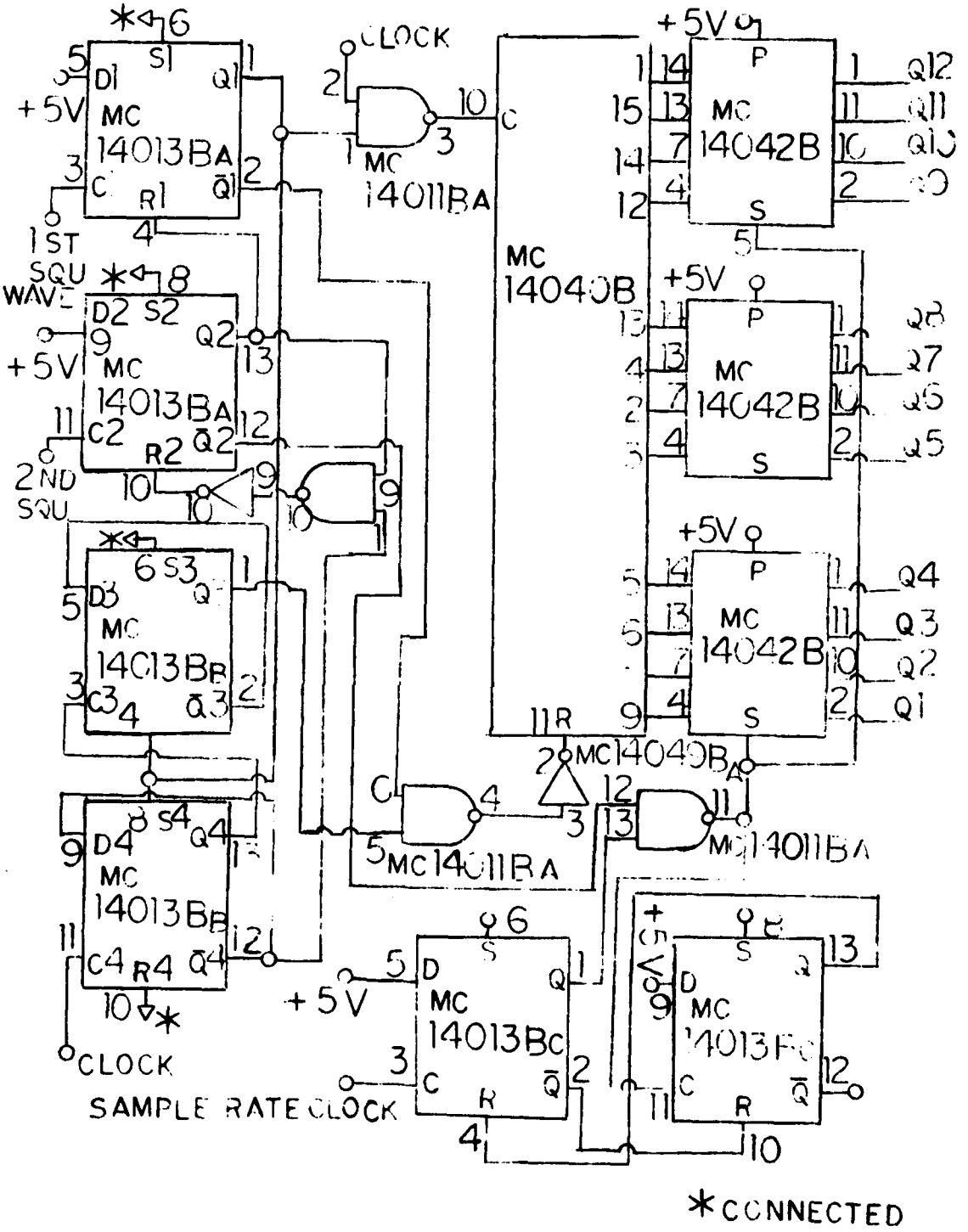

Digital phase meter schematic diagram

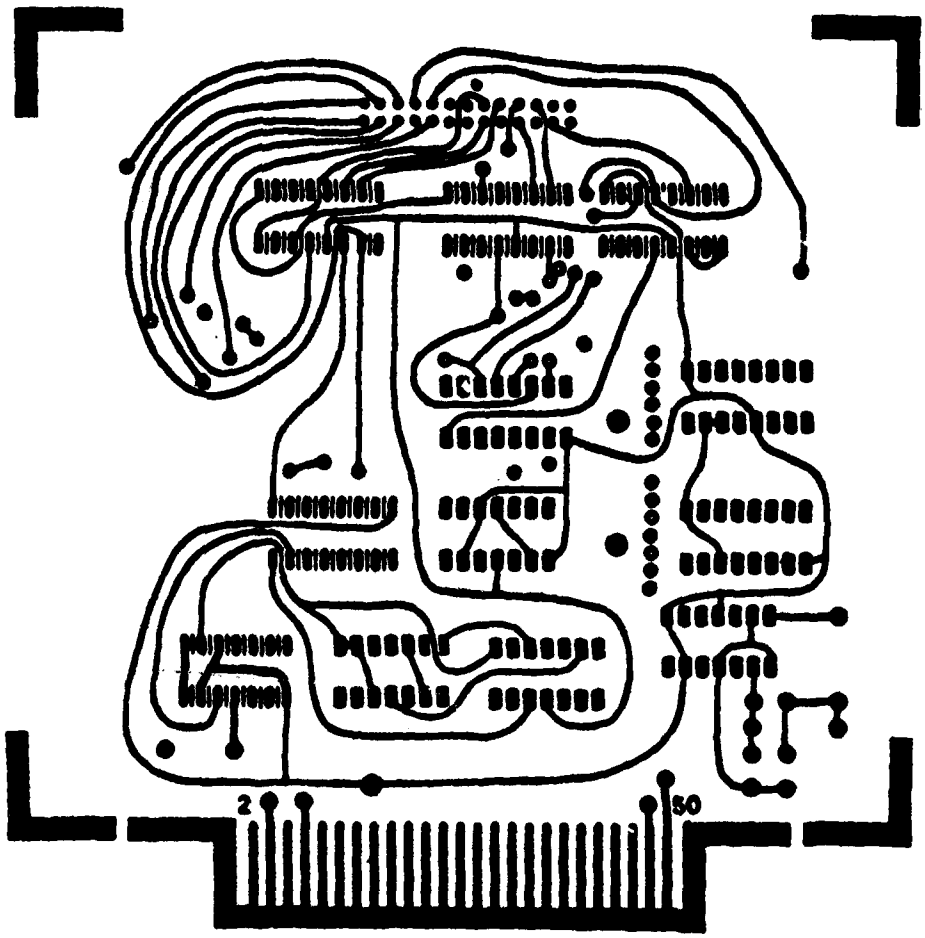

Digital phase meter board component side

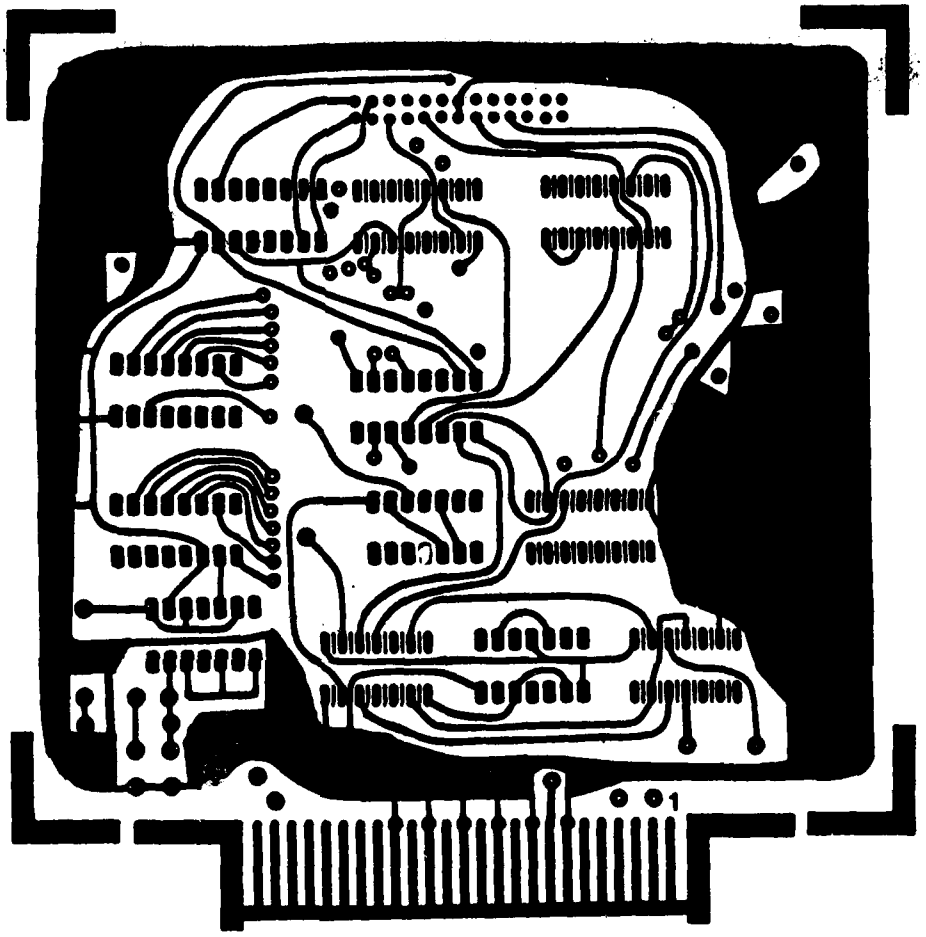

Digital phase meter board ground side

REGULATOR

MC 7824	+ 24 V REGULATOR	
MC 7812	+ 12 V "	
MC 7805	+ 5 V "	
MC 7924	- 24 V "	
MC 7912	- 12 V "	
C1	1 μF	CERAMIC CAPACITOR
D1	1N91 DIODE	
R1	220 Ω - 470 Ω	RN 60C PRECISION RESISTOR
LED1	LIGHT EMITTING DIODE	

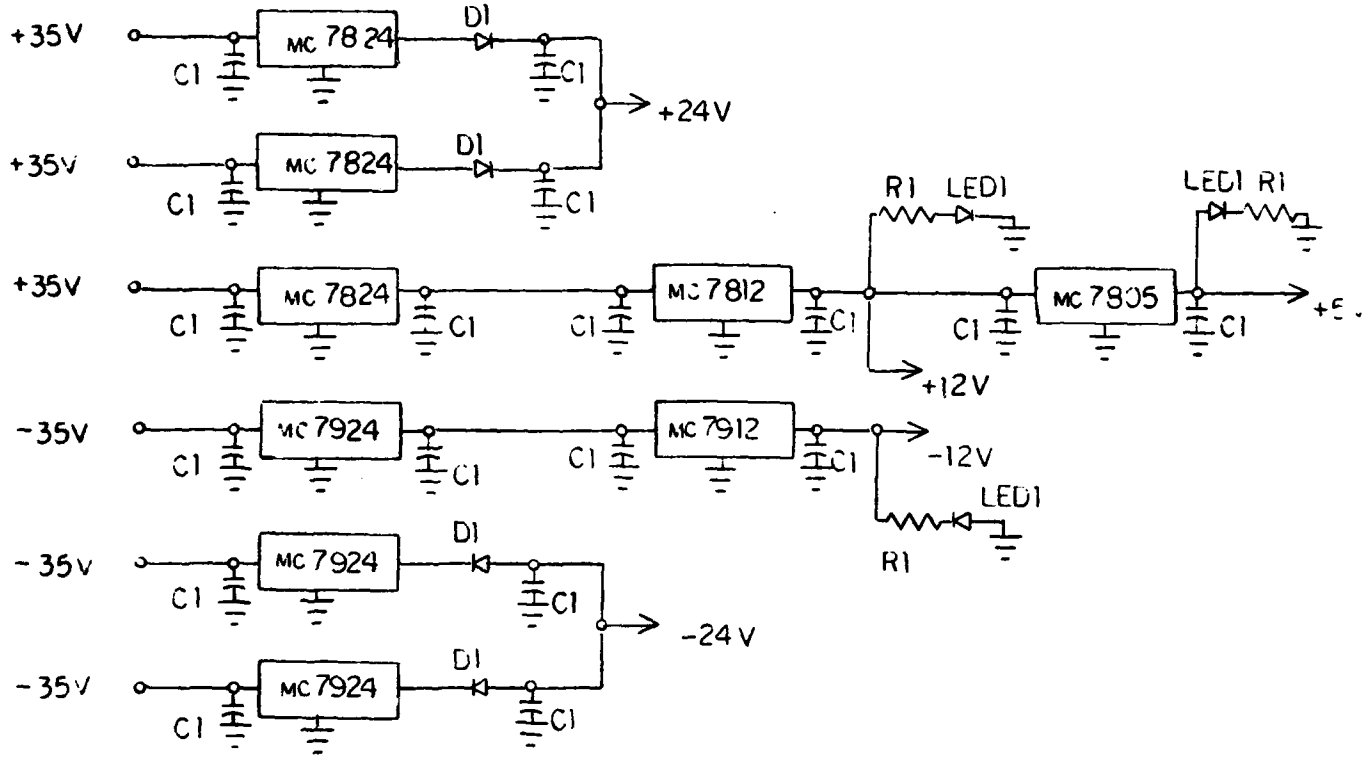

V_{CC} = +12 V

V_{EE} = −12 V

REVISIONS				
ZONE	LTR	DESCRIPTION	DATE	APPROVED

UNLESS OTHERWISE SPECIFIED DIMENSIONS ARE IN INCHES TOLERANCES ARE FRACTIONS DECIMALS ANGLES ± XX . XXX .

MATERIAL

FINISH

NEXT ASSY | USED ON

APPLICATION

DO NOT SCALE DRAWING

CONTRACT NO

APPROVALS	DATE
DRAWN T C	5/6/82
CHECKED	

B.A.T.

VOLTAGE REGULATOR

SIZE B | CODE IDENT NO. | DRAWING NO

SCALE | SHEET OF

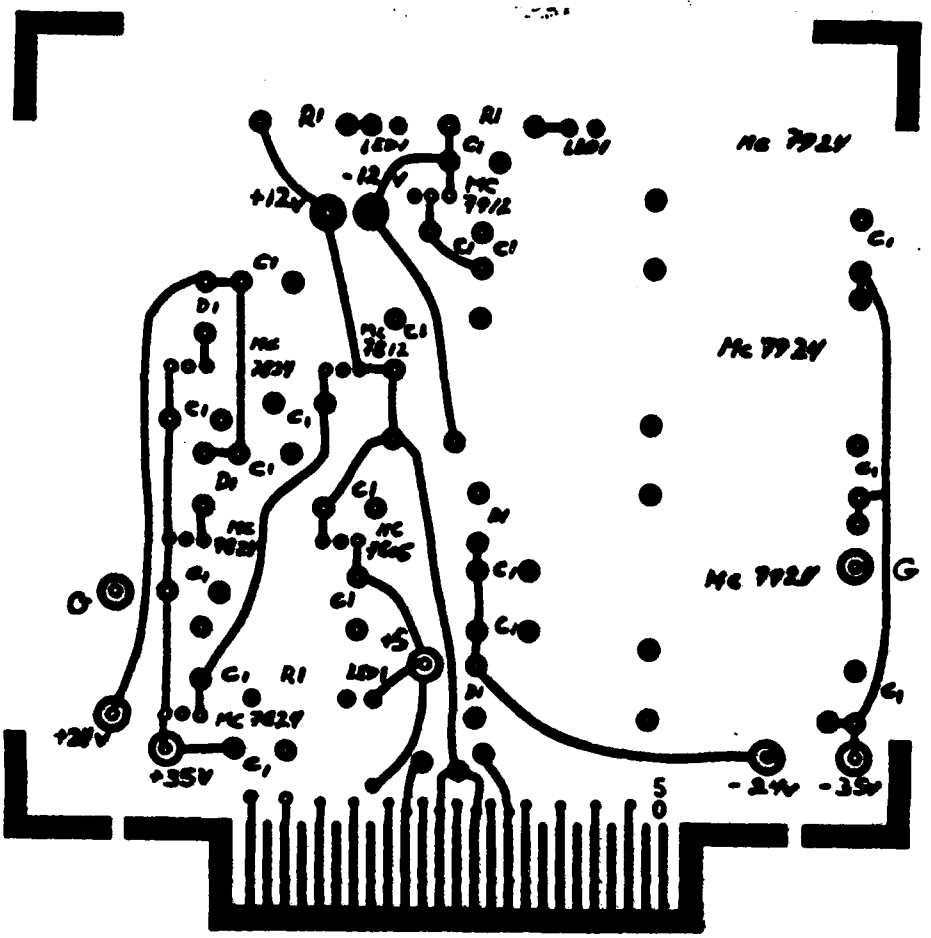

Voltage regulator board component side

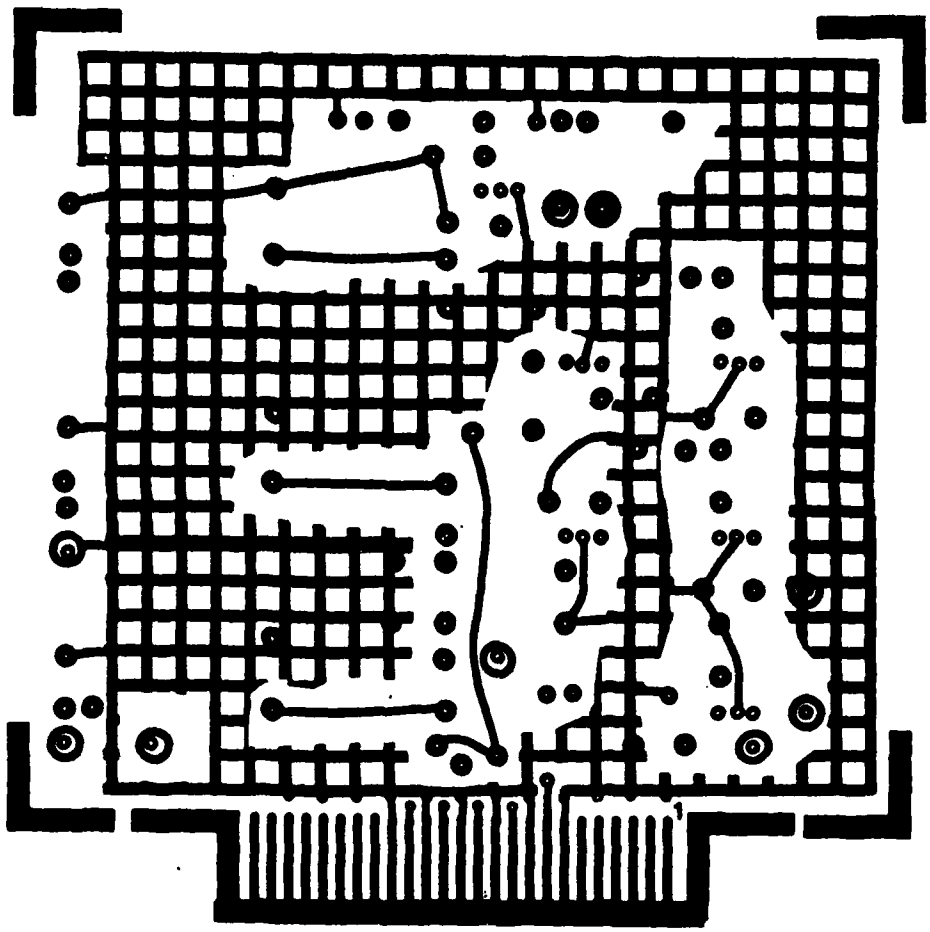

REGULATOR GROUND SIDE

Voltage regulator board ground side

Appendix VII

SPECIFICATIONS FOR THE ACOUSTIC COMPONENTS

This appendix contains information about the following acoustic components --

The electrostatic transmitter

The condenser microphone and preamplifier.

For more complete technical information about the microphone, pre-amplifier and supply see AR 1042 of the Aerophysics Lab and technical literature from Bruel and Kjaer.

ELECTROMAGNETIC TRANSMITTER

SCALE 1/1

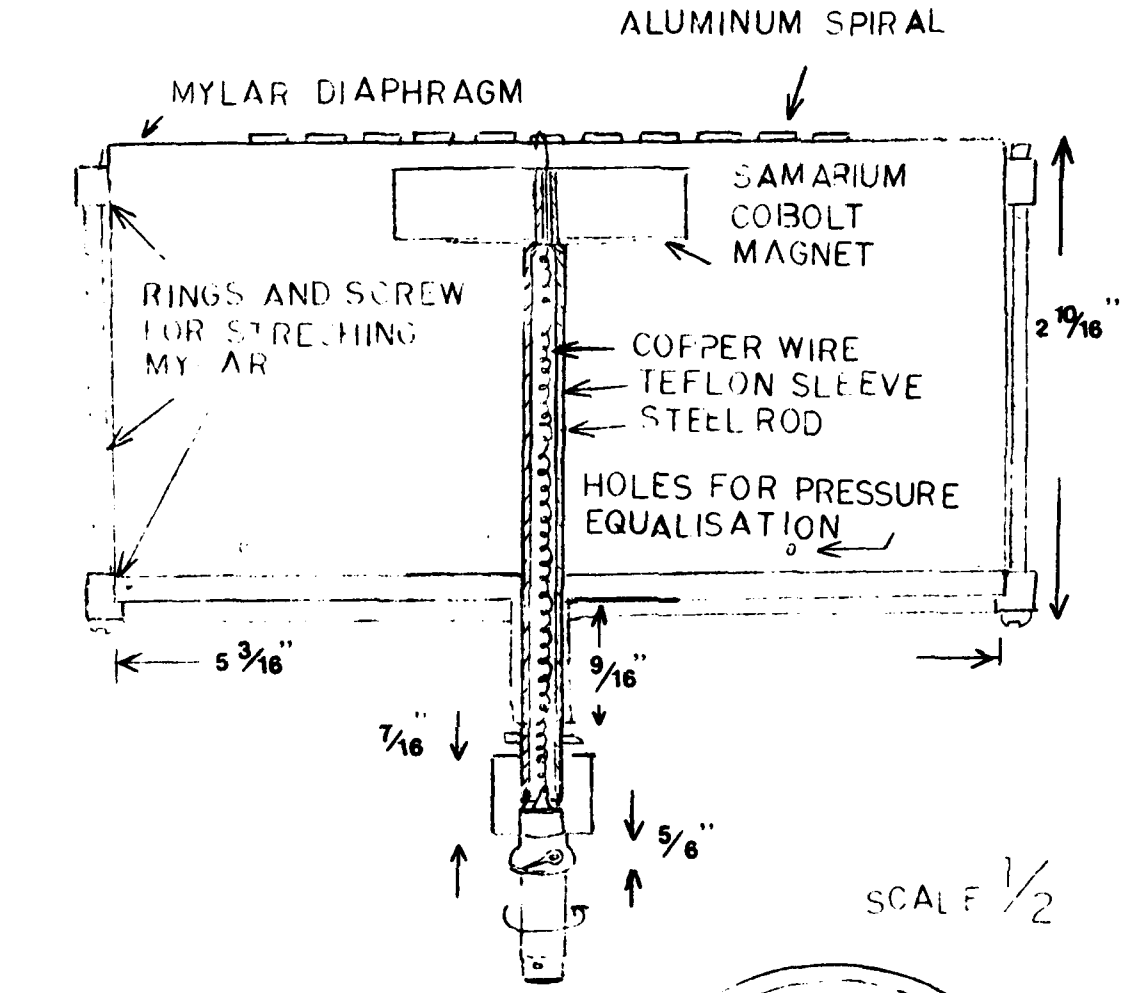

SCALE 1/2

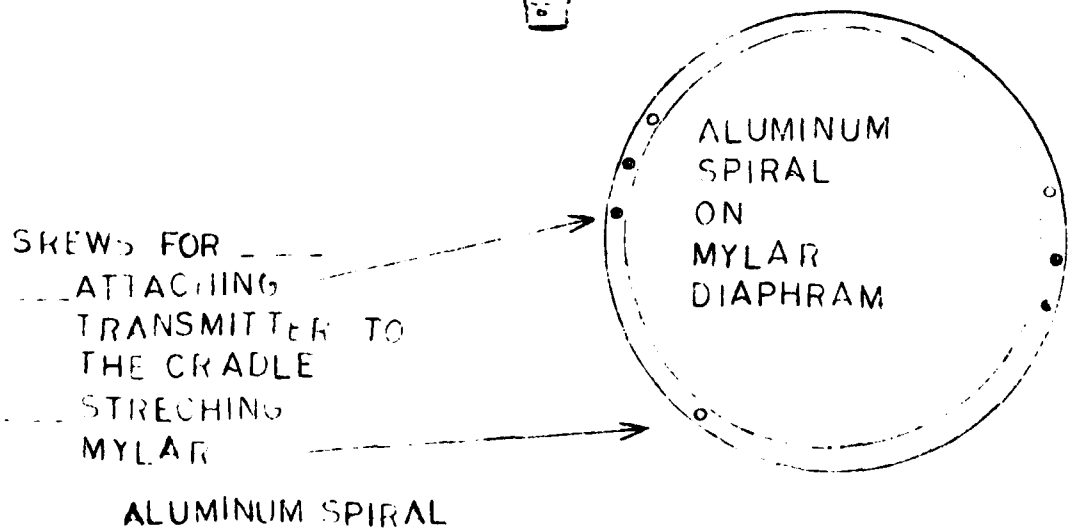

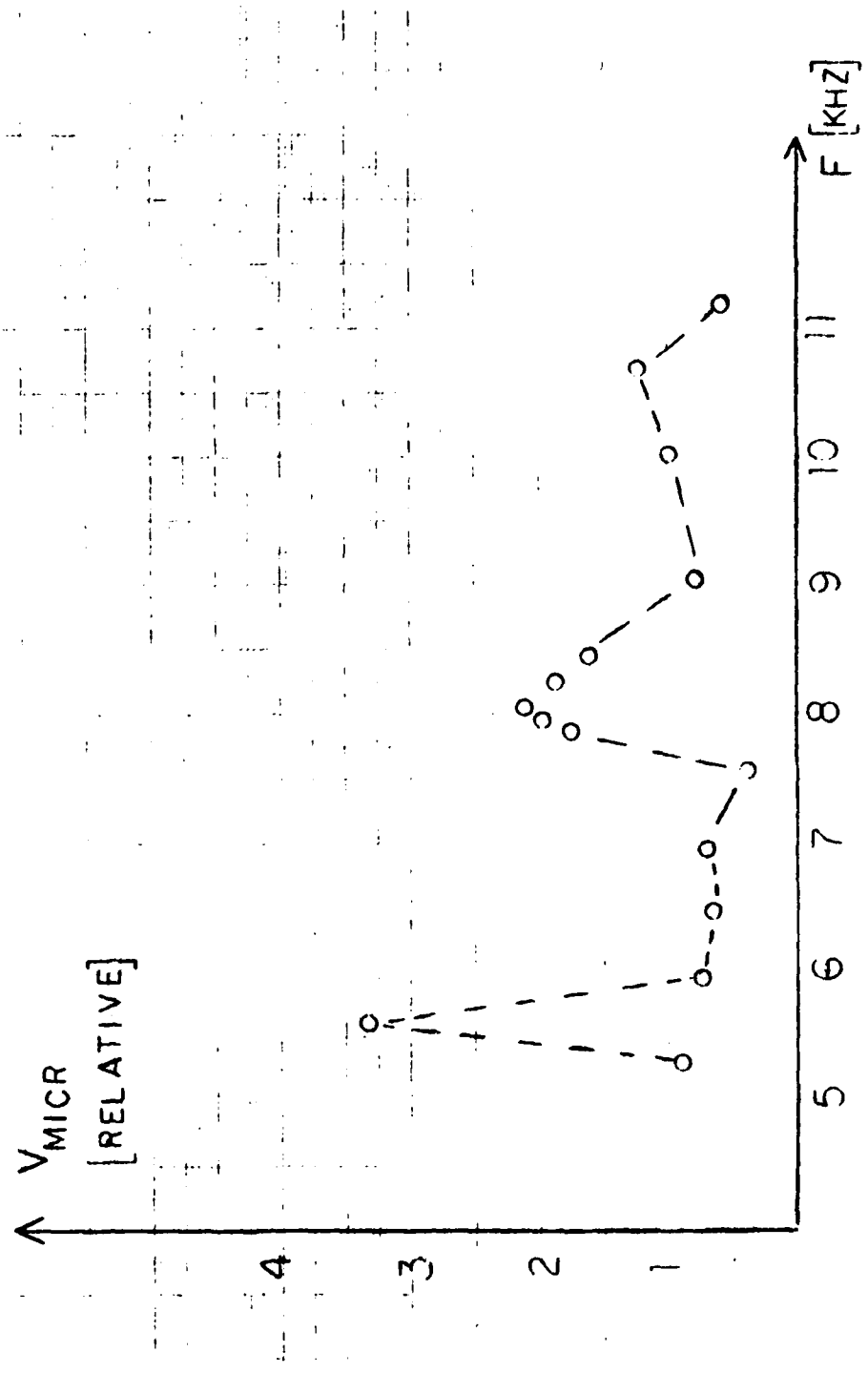

Frequency response of the transmitter

SPECIFICATIONS FOR THE ALUMINIZED MYLAR -

Lamotite T.M.
products

2909 East 79th Street, Cleveland, Ohio 44104 • Area Code 216 Phone: 883-8484 • Telex: 980-591

LAMOTAPE 951 - TENTATIVE PRODUCT DATA SHEET

Description: Electrical Shielding Tape

Construction: .00092" Polyester Film
.001" Aluminum Foil

951 Physical Data

Finished Weight:	3.04 oz./SY ± 5%
Specific Gravity:	2.028
Breaking Strength:	28 lbs. per inch width
Tensile Strength:	14,000 p.s.i.
Elongation at Break:	100%
Gauge:	0.002" ± 5%
Color:	Natural - Aluminum
Weight:	1,000 ft., 1" wide = 1.76 lbs.
Yield:	5.3 square yards per lb.

THE CONDENSER MICROPHONE

Some important data -

Microphone Type	Diameter	Nominal Polarization Voltage	0° Incidence Free Field Response ±2 dB (Hz)	Typical Random Incidence Response ±3 dB (Hz)	Pressure Response ± 2 dB (Hz)	Nominal Sensitivity (mV/Pa) (dB re 1 V/Pa)	Polarized Capacitance at 250 Hz (pF)
4165	[illegible]	[illegible]	2.5 – 20 k	2.0 – 10 k (with UA 0055)	[illegible]	[illegible]	18

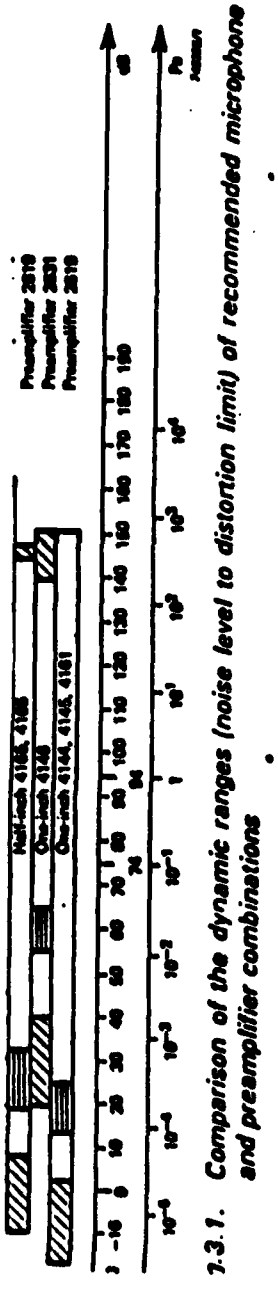

7.3.1. Comparison of the dynamic ranges (noise level to distortion limit) of recommended microphone and preamplifier combinations

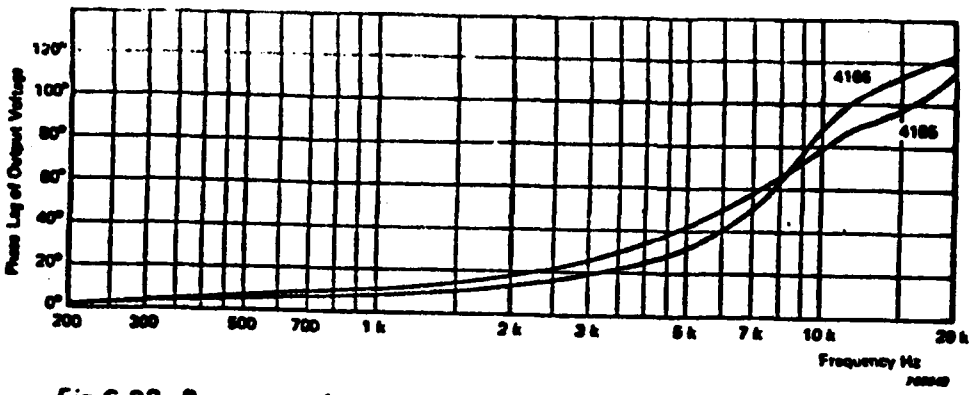

Fig.6.32. Pressure phase response of the half-inch microphones Types 4165, 4166

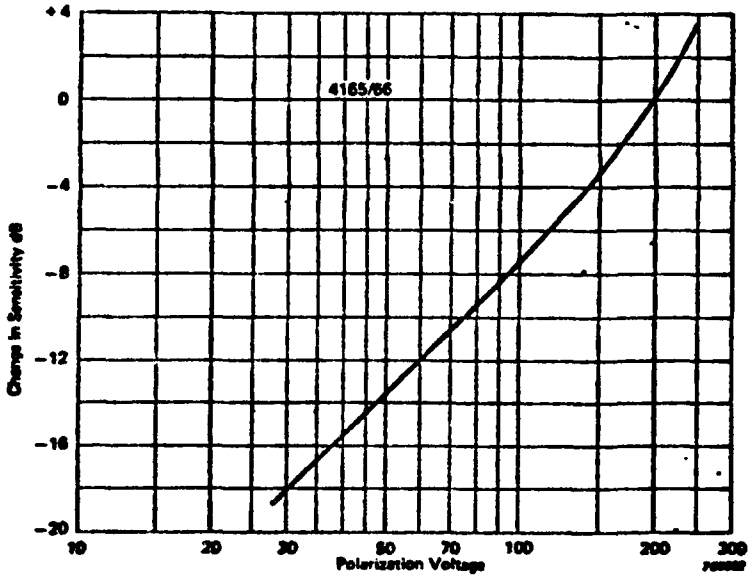

Fig.6.44. Sensitivity variation of half-inch microphones Types 4165 and 4166 at 250 Hz as a function of polarization voltage

(b)

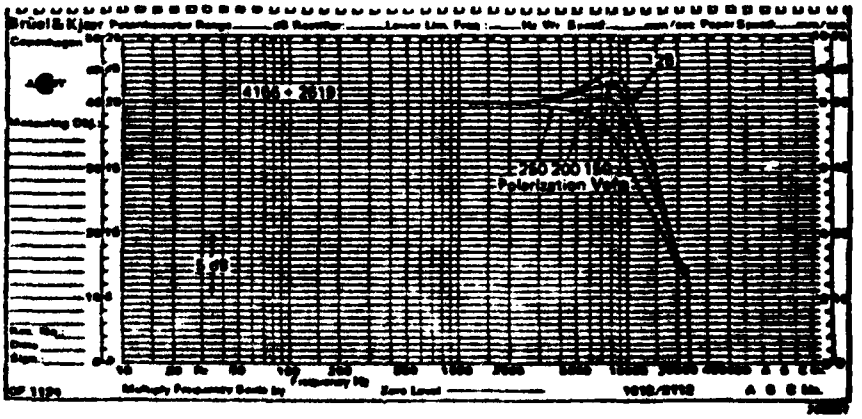

Fig.6.48. Effect of polarization voltage on frequency response of half-inch microphones
(a) Type 4165
(b) Type 4166

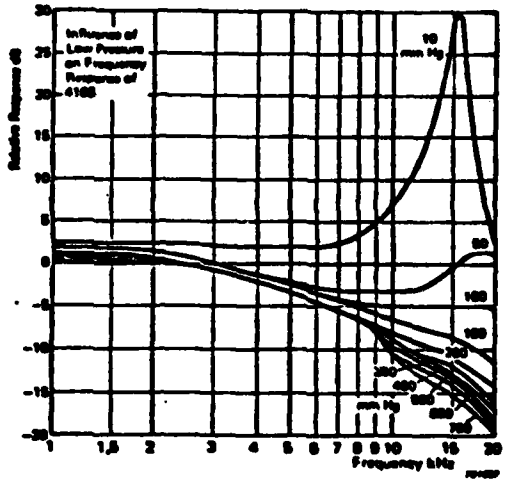

Fig.6.57. Effect of low pressure on frequency response of half-inch microphone

Type 4165
Note that 760 mm Hg = 1013 mbar = 1 atm

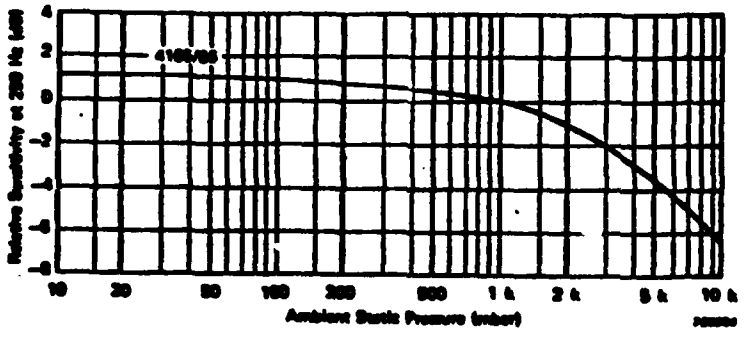

Fig.6.62. Variation of sensitivity at 250 Hz with ambient static pressure for half-inch microphones Type 4165

APPENDIX VIII

A POSSIBLE MODEL FOR PREDICTING THE EFFECT OF RADIATION HEATING IN THE ATMOSPHERE

The following estimate is based on numerical values given by Lichfield & Carlson (1967) for solar input and blackbody radiation.

Approximate surface area of chassis box:	Top	0.16 m^2
	Bottom	"
	Short sides	2 x 0.06 m^2
	Long sides	2 x 0.07 m^2
	Total	.58 m^2

Assume roughly one fifth of the chassis box is exposed to the sun

$$A_{exp.} \sim 0.1 \text{ m}^2$$

The power radiated in will be due to direct solar - and to infrared - radiation.

A typical solar input at float is 1200 w/m^2. Hence -

Power received from solar radiation ~ 120 W

A typical value for infrared radiation is given as 128 W/m^2 and hence, if assuming that the whole chassis box receives this, we have -

Power received from infrared radiation 65W

Thus, the total power input at float is 185 Watts.

The surface temperature is at equilibrium when the incoming energy equals the outgoing energy. The relationship between radiated power and temperature is -

$$E = ekT^4$$

- where e is the emissivity, a characteristic of the radiating surface and k is the Stefan-Boltzmann constant.

For a blackbody, where e is one, the outside surface temperature obtained from this power input would be about -30°C. For the aluminum chassisbox the exact emissivity would probably be about 0.1 thus lowering the surface temperature.

Assume for this simplified analysis that the chassisbox has no thermal resistance, but is covered by insulation with surface characteristics like a black body.

If the minimum tolerable temperature inside the chassisbox is +5°C the temperature difference across the insulation must be at least 35°C.

Since we have very low densities in the high atmosphere we ignore heat transfer by convection. Assuming pure conduction, with a linear temperature distribution, the heat transfer across the insulation is given by -

$$q = -k\frac{dT}{dx}$$

$$= (k/h)_{insulation}\,(T_{inside} - T_{outside})$$

- where h is the thickness of the insulation.

Now, the amount of heat we need to conduct out of the chassisbox is that dissipated in the electronic circuitry, given by

$$q_{diss} = |v| \cdot |i|$$

The total amount of power drawn by the instrument is approximately 27 watts but out of this some 13 watts is dissipated in conducting spiral of the transmitter. Thus the power dissipated in the box is about 14 watts.

Assuming that this power is conducted out evenly by the total box surface gives the heat transfer as 24 W/m^2. Note that the assumption of even distribution of heat transfer is unrealistic since it would require mixing of the air inside of the box by convection; but that we will use it here in lack of any better prediction.

Thus if we assume an insulation thickness of 2 cm's we get the following requirement to its' condutivity -

$$k_{ins} = \left(\frac{q}{\Delta T}\right)h$$

$$= (|v| \cdot |i| / \Delta T)h$$

$$\simeq 1.4 \cdot 10^{-2}\ W/m°C$$

This is about one tenth of the conductivity of the chassis box, and thus shows that insulation is necessary.

Although this analysis contains the theoretical framework for finding the necessary requirements of the insulation, it involves too many 'guesstimates' to yield meaningful information at present (eg - percentage of the chassisbox exposed to sunlight, emissisivity of the insulation, thermal resistance and heat transfer distribution in the chassisbox, etc.).

For the first launch time does not permit a closer analysis, so it was decided to insulate moderately and measure the temperature in the chassis box throughout the flight. However, the problems associated with controlling the temperature of the instrument should be carefully considered in the future.

APPENDIX IX

A THEORETICAL CALIBRATION CURVE

Equation 20 gives, with T_o = 25°C

T[°C]	V_s[Volts]	T[°C]	V_s[Volts]	T[°C]	V_s[Volts]
29	0.009	9	0.161	-11	0.864
28	0.005	8	0.182	-12	0.914
27	0.002	7	0.205	-13	0.966
26	0.001	6	0.229	-14	1.019
25	0.000	5	0.255	-15	1.073
24	0.001	4	0.282	-16	1.129
23	0.002	3	0.311	-17	1.186
22	0.005	2	0.341	-18	1.244
21	0.010	1	0.372	-19	1.304
20	0.015	0	0.405	-20	1.365
19	0.022	-1	0.440	-21	1.427
18	0.030	-2	0.475	-22	1.491
17	0.039	-3	0.513	-23	1.555
16	0.049	-4	0.552	-24	1.621
15	0.061	-5	0.592	-25	1.688
14	0.074	-6	0.633	-26	1.756
13	0.089	-7	0.677	-27	1.825
12	0.105	-8	0.721	-28	1.894
11	0.122	-9	0.767	-29	1.965
10	0.141	-10	0.815	-30	2.037

T[°C]	V_s[Volts]	T[°C]	V_s[Volts]	T[°C]	V_s[Volts]
-31	2.110	-49	3.489	-67	4.660
-32	2.183	-50	3.565	-68	4.706
-33	2.257	-51	3.640	-69	4.749
-34	2.332	-52	3.715	-70	4.789
-35	2.407	-53	3.788	-71	4.826
-36	2.483	-54	3.861	-72	4.860
-37	2.560	-55	3.932	-73	4.890
-38	2.637	-56	4.003	-74	4.918
-39	2.714	-57	4.071	-75	4.941
-40	2.791	-58	4.139	-76	4.961
-41	2.869	-59	4.205	-77	4.976
-42	2.947	-60	4.269	-78	4.988
-43	3.025	-61	4.331	-79	.996
-44	3.103	-62	4.391	-80	5.000
-45	3.181	-63	4.450	-81	4.999
-46	3.259	-64	4.506	-82	4.994
-47	3.336	-65	4.560	-83	4.984
-48	3.413	-66	4.611	-84	4.970

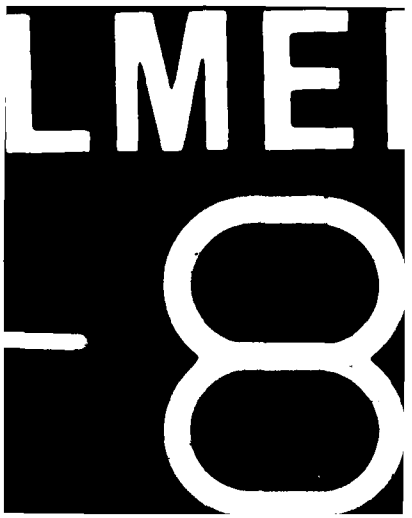
LME
8